Elemental analyses of diatom frustules

江本, 真理子

https://doi.org/10.15017/1654648

出版情報：九州大学, 2015, 博士（理学）, 課程博士
バージョン：
権利関係：全文ファイル公表済

Elemental analyses of diatom frustules

Mariko Emoto

Department of Earth and Planetary Sciences

Faculty of Sciences

Kyushu University

Contents

List of Figures i

List of Tables ii

Acknowledgements iii

Abstract iv

Chapter 1 Introduction: Recent studies on diatom frustules 1

1.1 Diatoms on the geochemical cycle in the oceans 1

1.2 Recent studies on diatom frustules 2

1.3 Separation of diatoms from the settling particles and sediments 3

1.4 Bering Sea 3

References 4

Chapter 2 Characterization of the settling particles and its implication on the vertical metal transportation 6

2.1 Introduction 6

2.2 Methods 7

2.2.1 Sediment trap samples 7

2.2.2 Compositional analysis 8

2.3 Results & Discussion 9

2.3.1 Elemental composition of the settling particles and comparison between the fractions 9

2.4 Conclusion 10

References 10

Figures 12

Chapter 3 Elemental analyses of diatom frustules based on aggregation-controlled dissolution kinetics 14

3.1 Introduction 14

3.2 Methods 16

3.2.1 Sediment trap samples 16

3.2.2 Compositional analysis 17

3.3 Results 18

3.3.1 Elemental composition of siliceous fraction and estimated composition of original diatom frustules 18

3.4 Discussion 19

3.4.1 Determination of elemental composition in fresh diatomaceous frustules 19

3.4.2. Comparison of the composition of diatom silica frustules with that of the upper crust 20

3.4.3. A box model to express the concentration of elements in diatom frustules 21

3.5 Conclusion 26

References 27

Tables and Figures 30

Chapter 4 Al-NMR studies of the settling particles collected in the highly diatom-productive Bering Sea: a new evidence for silicate dissolution/incorporation by diatoms 35

4.1 Introduction 35

4.2 Methods 36

4.2.1 Sediment trap samples 36

4.2.2 NMR spectroscopy 37

4.2.3 XRD spectrum 37

4.2.4 ICP-OES 38

4.3 Results & Discussion 39

4.3.1 ^{27}Al MAS NMR spectra of sediment trap samples 39

4.3.2. Variation of line intensities in spectra and its interpretation 40

4.3.3. Implication for presence of authigenic Al in diatom frustules 41

4.3.4. Support for diatomaceous dissolution/incorporation of metals in silicate minerals .. 42

4.4 Conclusion 43

References 43

Tables and Figures 46

Chapter 5 Problems on the chemical analyses of diatom frustules 51

5.1 Introduction 51

5.2 Methods 52

5.2.1 Sediment trap samples 52

5.2.2 Compositional analysis 52

5.3 Results & Discussion 53

5.4 Conclusion 54

References 54

Figures 56

Conclusion 57

List of Figures

Fig. 2.1 Proportion of elements dissolved in the HAc, HCl, and HF fractions. Circle graphs show the proportion at high, middle, and low productivity from the outside.

Fig. 2.2 Concentration ratios of elements against silicon (M/Si) in settling particles, compared to those of the upper crust (Rundnick et al., 2004).

Fig. 3.1 Map shows the location of studied sites: Station AB (53°5'N, 177°W) and Station SA (49°N, 174°W).

Fig. 3.2 Concentrations of elements in siliceous fractions plotted against opal flux in an order of periodic table. The elements whose concentrations are close to the lower detection limits are not shown.

Fig. 3.3 M/Si in diatom frustules vs M/Si in the upper crust. The solid line shows 1:1 relationship and dotted line 1:50 relationship.

Fig. 3.4 Box model structures of silicon (a) and terrigenous elements (b). See text for details.

Fig. 4.1 Map shows the location of studied sites: Station AB (53°5'N, 177°W, water depth 3197 m).

Fig. 4.2 ^{27}Al MAS NMR spectra of the sediment trap samples and de-convoluted lines.

Fig. 4.3 XRD patterns of settling particles. Q, quartz; Cal, calcite; M, muscovite; K, kaolinite; Ch, chlorite; F, feldspar; H, halite.

Fig. 4.4a Al concentration in settling particles at various opal flux.

Fig. 4.4b Relation of Al concentration in settling particles and area ratio of sharp peak (line 2).

Fig. 5.1 Amounts (μg) of elements leached in six fraction (A-F) from one gram samples.

List of Tables

Table 3.1 Concentration (μg/g) of diatom frustules estimated from the asymptotic values in Figure 3.1.

Table 4.1 Peaks observed in ^{27}Al MAS NMR spectra of sediment trap samples.

Table 4.2 Al concentration, opal flux and residual ratio for sediment trap samples.

Acknowledgements

This thesis was completed in the course of the running studies at the laboratory of Inorganic Geochemistry for the Biosphere, while I was in doctoral course of Department of Earth and Planetary Sciences, Graduate School of Science, Kyushu University. I am deeply grateful to my supervisor, Prof. Tasuku Akagi at this University, for long-term support. His guidance, encouragement and advice made this work go forward enormously. I would like to thank Assoc. prof. Junichiro Ishibashi and Prof. Takushi Yokoyama at this University, and Prof. Yoshiki Sohrin at Kyoto University. Their constructive advice and comments have been a great help in discussion of the paper.

I would like to thank Prof. Kozo Takahashi and Dr. Makio Honda at Japan Marine Science and Technology Center for their generous offer of invaluable sediment trap samples, Dr. seiichiro Uehara at this University for his help in the XRD analysis and Dr. Mayumi Etoh for her help in acquisition and handling of NMR data. Last of all, I acknowledge support by all faculty members at the department and encouragement of past and present members of the laboratory.

Abstract

Diatoms are one of the most important planktonic phases in the oceans accounting for more than a half the oceanic primarily production. Because of difficulty in separating diatom frustules from silicate minerals chemically and physically, diatom frustules have been analytically-forbidden entities. Diatom frustules have been assumed to be pure opal without any analytical proof. If they are not pure opal, their potential to contribute to the oceanic cycles of elements other than silicon should not be overlooked. In this dissertation, it is shown how impure diatom frustules are.

Earlier attempts to elucidate chemical composition of diatom frustules are briefly surveyed. It is shown that there is no evidence in analytical chemistry to conclude that diatom frustules are pure opal. A new method based on dissolution kinetics is introduced and the consequence of the oceanic cycles of rare earth elements is described. To understand the basic characteristics of settling particles, sediment trap samples collected form the diatomaceously productive Bering Sea is analyzed with a sequential leaching technique. This chapter introduces chemical characterization of settling particles and shows what elements pertain to carbonate, oxide, and siliceous fractions. The dissolution kinetics is further applied to the composition of the siliceous fractions to estimate the composition of diatom frustules. It is shown that diatom frustules contain many metals at the concentrations greater than one hundredth of those in terrigenous silicate minerals.

The composition was further explained in terms of metal-silicic acid complex formation and dissolved metal concentration in the deep water by using a box model. To endorse the estimated composition of diatom frustules, chemical speciation of aluminum, a representative of terrigenous elements, in sediment trap samples has been carried out using nuclear magnetic resonance spectroscopy. It is shown that most of aluminum of settling particles is in siliceous fraction and is chemically different states from those in clay minerals. The results strongly indicate that the metal elements of the estimated composition of diatom frustules are not due to contamination with terrigenous matter, but due to indigenous metal absorbed physiologically by diatoms. To address an implication relevant to analytical chemistry of diatom frustules, the conventional analytical method of diatom frustules using an alkaline solution is revisited and it is shown that the method tends to overlook most of metal elements in diatom frustules.

To finalize the dissertation, some implications of this study are addressed in relevance to marine chemistry. It is stated that diatom frustules should be one of the most important carriers of elements from the surface to the deep water in the oceans.

Chapter 1

Introduction: Recent studies on diatom frustules

1.1. Diatoms and the geochemical cycle in the oceans

Diatoms, one of the phytoplankton, account for about half the total primary productivity in the oceans (de la Rocha, 2006) and have a potential to play an important role on elemental circulation in the oceans. A characteristics of diatoms is that they have siliceous frustules though size and shape vary depending on species. Hence, productivity of diatoms is limited by silicon concentration of surface water. In the North Pacific and Antarctic Oceans where upwelling currents supply silicate and other nutrients, the diatomaceous productivity is extremely high. Radiolaria, a zooplankton, competes with diatoms because they also have siliceous skeleton, but fertile diatoms are predominant in the regions.

Diatoms aggregate in the surface water probably being caused by sticky organic protective coating and long spines, then aggregates settle through a water column. Sediment trap is a method to collect the aggregates, called settling particles, and to observe biogenic silica, carbonate, and organic flux transported to the ocean floor. In the case of the Bering Sea, which is known as one of seas with the highest primary production in the world oceans, biogenic silica usually account for approximately 60% of the settling particles and diatoms are the major constituents of biogenic silica (Takahashi et al., 2002).

Vertical profile of dissolved silica in the oceans is classified to a nutrient type and it is explained by a diatomaceous contribution: silicic acid is consumed by diatoms at the surface and released from settling particles at the deep water. Tréguer et al. (1995) discussed the silicon

cycle in the world ocean and estimated that 97% of biogenic silica was dissolved during settling toward sea floor and finally recycled. Generally, diatoms contribute to vertical profiles of some elements (Si, N, P, and C) through dissolution of the frustules and organic matter. Some of trace essential elements showing nutrient type profiles (e.g. Fe, Cu, Zn) may be explained by similar processes, but the profiles cannot be explained only by dissolution of the organic matter. Moreover, there is no quantitative explanation why the profiles of rare earth elements (REEs) are of a nutrient type, though REEs are not nutrient elements.

1.2. Recent studies on diatom frustules

One of the reasons for preventing interpretation of vertical profiles is that diatom frustules are regarded as pure opal. However, Akagi et al. (2011) reported that diatom frustules contain REEs at significant concentration as impurity and that they are main carriers of REEs in a water column and the REEs in diatom frustules are released to seawater in the course of dissolution of the frustules. This discovery further has led to the identification of carbonate as a REE scavenger from water columns (Akagi et al., 2014). In other words REEs in silicate minerals should somehow be taken in by diatoms: probably through dissolution of silicate minerals by diatoms.

These studies suggest that diatom frustules may contain various elements such as aluminum and titanium, typical terrigenous elements. Akagi et al., (2013) showed aluminum, which is trivalent ion similar to REEs, exists all around in diatom frustules based on SEM image. If diatom frustules contain various elements, they have potential of contribute to vertical profiles in the oceans.

1.3. Separation of diatoms from the settling particles and sediments

A problem in chemical analyses of sediment trap samples and sediments is difficulty in separation between diatom frustules (and other biogenic silica) and terrigenous matter like clay minerals because both are silicate. Shemesh et al. (1988) tried to separate diatoms from clay minerals carefully by physical separation and chemical cleaning while monitoring Ge/Si ratio, but they concluded due to the Fe and Al correlation that contamination of clay minerals might remain even when Ge/Si ratio is low. In addition to that, Ellwood and Hunter (1999) premised that Al and Fe came from clay in their discussion, though they report existence of Zn in diatom frustules according to difference of behavior of Al and Fe with time during analysis. Kamatani (2000) reviewed difficulty in analyses of diatoms such as difference in dissolution rate of diatom frustules with an alkaline solution and reaction time.

According to Akagi et al. (2013) and Beck et al. (2002) which reported Al existence in natural and cultured diatom frustules respectively, it is not absolutely necessary that Al is considered as influence of contamination. However, it is noted that a border between diatom frustules and clay minerals is quite ambiguous.

1.4. Bering Sea

Akagi et al. (2011) developed the aggregation-controlled dissolution kinetics of diatomaceous frustules to explain the hyperbolic relationship observed between elemental concentration and opal flux, and concluded that asymptotic values at infinite diatom productivity (>200 mg m^{-2} day^{-1}) should correspond to the original composition of diatom frustules. The rationale is siliceous matter in settling particles at extremely high diatomaceous

production form mega-aggregates and keeps frustule composition unaltered as a result of increase in their settling velocity and of decrease in surface area per opal mass. The Bering Sea is known as one of the highest primary productivity region in the world, and sediment trap samples when opal flux is high above >200 mg m^{-2} day^{-1} can be obtained in the Bering Sea.

References

Akagi, T., Fu, F.-f., Hongo, Y. and Takahashi, K. (2011) Composition of rare earth elements in settling particles collected in the highly productive North Pacific Ocean and Bering Sea: Implications for siliceous-matter dissolution kinetics and formation of two REE-enriched phases. *Geochimica et Cosmochimica Acta* **75**, 4857-4876.

Akagi, T., Emoto, M., Tadkada, R. and Takahashi, K. (2013) Diatom frustule is an impure entity: Determination of biogenic aluminum and rare earth element composition in diatom opal and its implication on marine chemistry, Diatoms, Diversity and Distribution, Role in Biotechnology and Environmental Impacts. Nova Science Publishers, Inc., New York, p. 127.

Akagi, T., Yasuda, S., Asahara, Y., Emoto, M. and Takahashi, K. (2014) Diatoms spread a high εNd-signature in the North Pacific Ocean. *Geochemical Journal* **48**, 121-131.

Beck L., Gehlen M., Flank A. M., Van Bennekom A. J. and Van Beusekom J. E. E. (2002) The relationship between Al and Si in biogenic silica as determined by PIXE and XAS, *Nuclear Instruments and Methods in Physics Research Section B: Beam Interactions with Materials and Atoms*, **189**, 180-184.

de la Rocha C. L., (2006) The biological pump. In *The Ocean and Marine Geochemistry. Treatise on Geochemistry*, vol. 6 (ed. H. Elderfield). Elsevier-Pergamon, Oxford.

Ellwood M. J. and Hunter K. A. (1999) Determination of the Zn/Si ratio in diatom opal: a method for the separation, cleaning and dissolution of diatoms. *Mar. Chem.* **66**, 149-160.

Shemesh A., Mortlock R. A., Smith R. J. and Froelich P. N. (1988) Determination of Ge/Si in marine siliceous microfossils: Separation, cleaning and dissolution of diatoms and radiolarian, *Marine Chemistry*, **25**, 305-323.

Takahashi K., Fujitani N. and Yanada M. (2002) Long term monitoring of particle fluxes in the Bering Sea and the central subarctic Pacific Ocean, 1990-2000. *Progr. Oceanogr.* **55**, 95-112.

Tréguer P., Nelson D. M., Van Bennekom A. J., DeMaster D. J., Leynaert A. and Quéguiner B. (1995) The silica balance in the world ocean: a reestimate. *Science* **268**, 375-379.

Chapter 2

Characterization of the settling particles and its implication on the vertical metal transportation

2.1. Introduction

Settling particles play an important role in vertical transportation in the oceans. Settling velocity of particles is about 160 m day^{-1} (Honjo and Manganini, 1993; Honjo et al., 1995; 1999), and in other words it takes only 3-4 weeks to reach sea floor of 4 km depth. Particulate matter is produced by biological and inorganic processes in surface water, and reacts with sea water while settling though a water column. In general, most of particles dissolve in sea water before reaching sea floor and elements composing the particles recycle to the surface. According to Kawahata et al. (1998) who investigated vertical flux of settling particles in West Equatorial Pacific Ocean, ratio of total mass flux escaping dissolution and reaching sea floor is less than 20% at the depth of 1600 m.

Settling particles can be divided into four categories:

i. Biogenic silica (frustules of diatom and radiolaria)
ii. Carbonate (tests of coccolith and foraminifera, and hydrogenous material)
iii. Organic matter
iv. Terrigenous matter.

The amount of total mass flux of settling particles in the oceans or on seasons depends on productivity. If productivity is high, dead plankton skeletons are intertwined and form large aggregation. As a result of increasing settling velocity, it is considered that amount of

transported matter to the sea floor increases compared to that in normal season. In the case of the Bering Sea where this study investigated, most important contributor of the flux is diatoms (Takahashi et al., 2002), therefore, opal flux can be assumed as a parameter of the diatomaceous productivity.

Recently, Akagi et al. (2011) developed the aggregation-controlled dissolution kinetics of diatomaceous frustules to explain the hyperbolic relationship observed between elemental concentration and opal flux, and concluded that asymptotic values at infinite diatom productivity should correspond to the original composition of diatom frustules. The rationale is siliceous matter in settling particles at extremely high diatomaceous production form mega-aggregates and keeps frustule composition unaltered as a result of increase in their settling velocity and of decrease in surface area per opal mass.

In this study, elemental composition of silicate minerals, oxide, and carbonate was compared in order to investigate which phases may be responsible for the transportation of elements.

2.2. Methods

2.2.1. Sediment trap samples

Sediment trap samples were collected at Station AB (53°5'N, 177°W, water depth 3197 m) in the Aleutian Basin of the Bering Sea and Station SA (49°N, 174°W, water depth 5406 m) in the central subarctic Pacific (Fig. 2.1). To collect the samples a PARFLUX Mark 7G-13 time-series sediment trap with 13 rotary collections was deployed approximately 600 m above the seafloor.

Before the further analysis a sample was immersed in a storage solution to preserve the biogenic matter. The storage solution (5% formaldehyde solution) was prepared by mixing

North Pacific deep seawater, formaldehyde and sodium borate buffer to adjust the pH from 7.6 to 8.0. Subsets of the samples were subjected to routine analysis for opal, calcium carbonate, and organic carbon contents, following the procedure described in Takahashi et al. (2002). Ten samples from Station AB and one sample from Station SA were analyzed for the elemental composition.

2.2.2. Compositional analysis

Settling particles separated from the formaldehyde storage solution by centrifugation were washed with 6 ml of ethanol and 3 ml of Milli-Q water, and freeze-dried. 10 mg of the dried sample (4 mg for AB-20 #20) was treated with 10 ml of 40% acetic acid solution at 40°C for 25 minutes. The supernatant solution was separated from residue (HAc residue) by centrifugation. After the solution was evaporated to dryness, HNO_3 solution and water were added. Then, 10 ml of 3% hydrochloric acid was added to the HAc residue. The solution was separated by centrifugation and evaporated and HNO_3 solution and water were added. The treatment with acetic acid and hydrochloric acid solutions is supposed to dissolve carbonates and oxides, respectively and the solutions were named HAc and HCl fractions, respectively. The HCl residue, mainly consisting of siliceous matters, was transferred to a Teflon vessel using 1 g of 68% nitric acid. 1 g of 70% perchloric and 1 g of 35% hydrofluoric acids were added to the vessel and the residue was decomposed completely by heating for 90 minutes. After evaporation, HNO_3 solution and water were added and the final solution was named HF fraction. Three final solution (approx. 1 N HNO_3) were determined using inductivity coupled plasma mass spectrometry (ICP-MS; HP4500, Agilent Co., Ltd.). To avoid memory error by using a multi element standard solution at high concentrations, the calibration was carried out against a JB-3 decomposed solution with the known element concentration.

2.3. Results & Discussion

Circle graphs (Fig. 2.1) show the proportion of elements dissolved in the three fractions (HAc, HCl, and HF). Carbonate, oxide and silicate phases are typically dissolved by acetic acid, hydrochloric acid and mixed acid including fluoric acid, respectively. Samples were divided into 3 groups with respect to diatom productivity; high productivity (opal flux >200 mg m^{-2} day^{-1}, n=5), middle productivity (opal flux 50-200 mg m^{-2} day^{-1}, n=3), low productivity (opal flux <50 mg m^{-2} day^{-1}, n=3).

In many elements (Li, Be, Mg, Al, Sc, Ti, V, Cr, Fe, Co, Cu, Zn, Ga, As, Rb, Y, Zr, Nb, Sn, Sb, Cs, REEs, Hf, Ta, W, and Th), the HF fraction accounts for the greatest proportion regardless of productivity compared with the other two fractions. HCl fraction explains the greatest proportion of Ba and Ag; the HAc fraction of Na, K, Ca, Mn, Ni, Sr, Pb, Bi, and U. The proportions of elements in the HF fraction do not change significantly depending on diatom productivity.

Concentration ratios of elements against silicon (M/Si) in settling particles are compared to those of the upper crust (Rundnick et al., 2004) in Fig. 2.2. The overall patterns of elements when productivity is high are almost the same as that of middle productivity group. Although the ratios for the low productivity group are higher by a factor of 3 to 5 than those for the high productivity group, the overall pattern is similar to the others. This is simply explained by: most of elements are dominantly contained in the HF fraction; Si is considered to be more intensively dissolved than most of other elements during the settling through water columns in a sample with lower productivity based on the dissolution kinetics (Akagi et al., 2011).

2.4. Conclusions

It is concluded that 1) the settling particles transport a variety of elements to the seafloor, 2) the overall pattern is distinct from that of the upper crust, and 3) the most of element concentrated in the siliceous fraction (HF fraction) with similar abundance pattern. In this thesis, the composition of siliceous fraction will be more deeply discussed.

Reference

Akagi T., Fu F.-F., Hongo Y. and Takahashi K. (2011) Composition of rare earth elements in settling particles collected in the highly productive North Pacific Ocean and Bering Sea: implications for siliceous-matter dissolution kinetics and formation of two REE-enriched phases. *Geochim. Cosmochim. Acta* **75**, 4857-4876.

Honjo S. and Manganini S. J. (1993) Annual biogenic particle fluxes to the interior of N Atrantic Ocean; studied at 34° N21°W and 48°N21°W. *Deep-Sea Res.* **40**, 587-607.

Honjo S., Dymond J., Collier R. and Manganini S. J. (1995) Export production of particles to the interior of the Arabian sea. *Deep-Sea Res.* **42**, 831-870.

Honjo S., Dymond J., Prell W. and Ittekkot V. (1999) Monsoon-controlled export fluxes to the interior of the Arabian sea. *Deep-Sea Res.* **46**, 1859-1902.

Kamatani, A. (2002) Measuring biogenic silica of marine samples: its situation and prospect. *J. Oceanogr. Soc. Japan* **9**, 143-159.

Kawahata, H., Yamamuro, M. and Ohra, H. (1998)Oceanologica Acta, 21, 521-532.

Rudnick R. L. and Gao S. (2004) Composition of the continental crust. In *The Crust. Treatise on Geochemistry*, vol. 3 (ed. R. L. Rudnick). Elsevier-Pergamon, Oxford.

Takahashi K., Fujitani N. and Yanada M. (2002) Long term monitoring of particle fluxes in the Bering Sea and the central subarctic Pacific Ocean, 1990-2000. *Progr. Oceanogr.* **55**, 95-112.

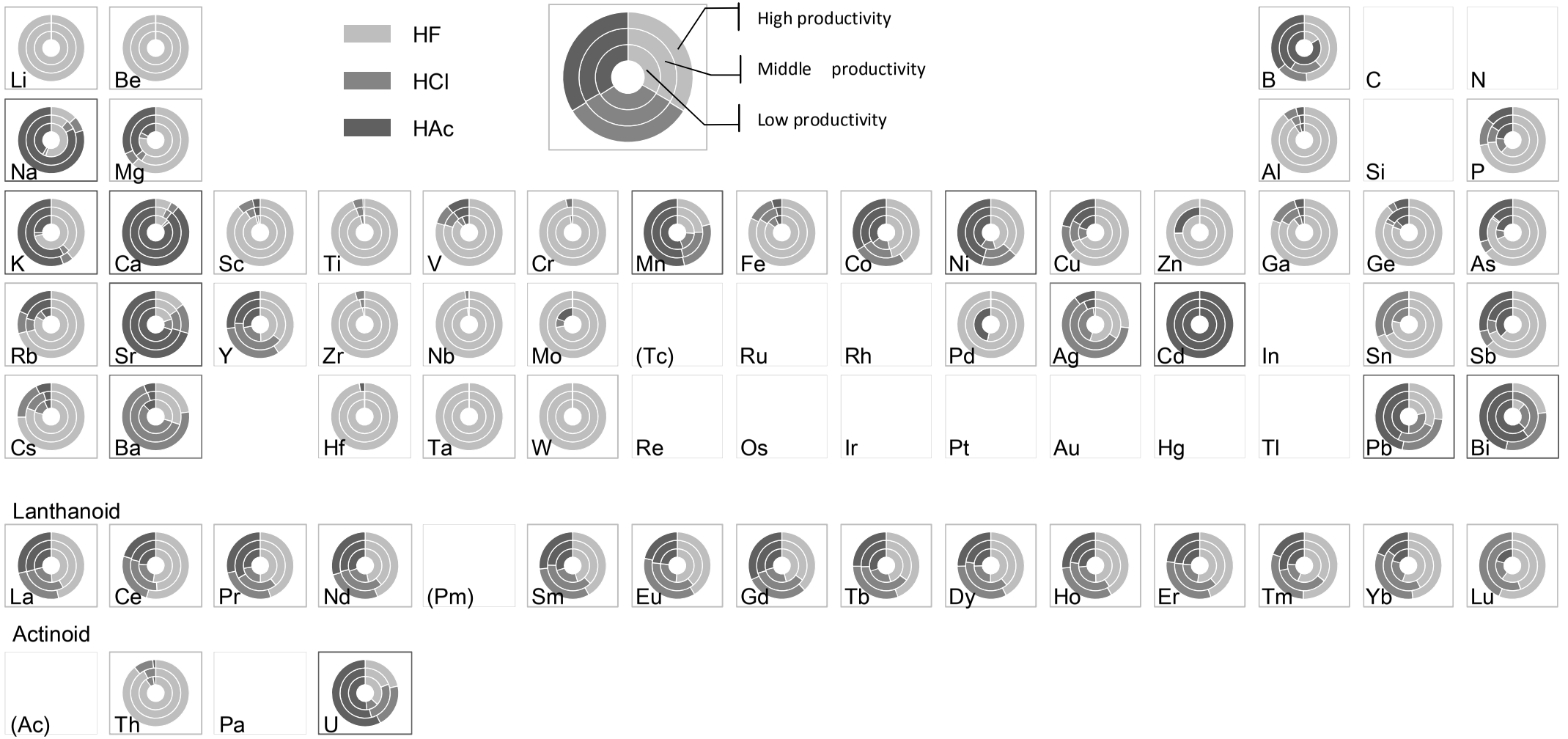

Fig. 2.1 Proportion of elements dissolved in the HAc, HCl, and HF fractions. Circle graphs show the proportion at high, middle, and low productivity from the outside.

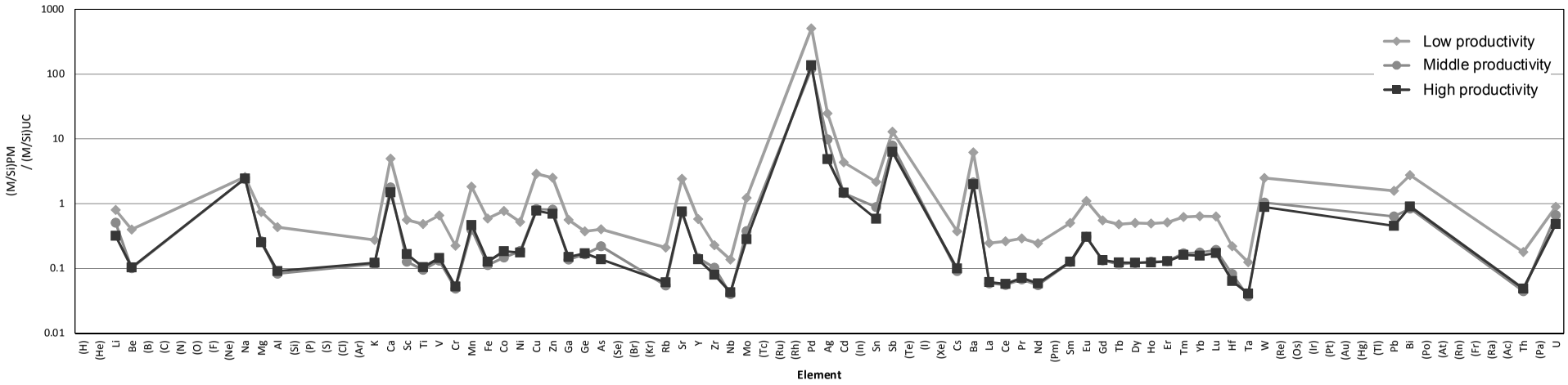

Fig. 2.2 Concentration ratios of elements against silicon (M/Si) in settling particles, compared to those of the upper crust (Rundnick et al., 2004).

Chapter 3

Elemental analysis of diatomaceous frustules based on aggregation-controlled dissolution kinetics

3.1. Introduction

Settling particles are important when discussing the vertical profiles of dissolved components in the oceans, because they play a role in vertical material transportation contributing to addition/removal of dissolved elements. Diatoms are responsible for about half the total on primary productivity in the oceans (de la Rocha, 2006), and their frustules constitute one of major substances of settling particles together with $CaCO_3$, organic matter and clay. Diatom frustules may have a potential to contribute to the ocean material cyclings, but their chemistry other than amorphous silicate is poorly known.

Recently, Akagi et al. (2011) developed the aggregation-controlled dissolution kinetics of diatomaceous frustules to explain the hyperbolic relationship observed between elemental concentration and opal flux, and concluded that asymptotic values at infinite diatom productivity should correspond to the original composition of diatom frustules. The rationale is siliceous matter in settling particles at extremely high diatomaceous production form mega-aggregates and keeps frustule composition unaltered as a result of increase in their settling velocity and of decrease in surface area per opal mass.

By adopting the asymptotic REE composition, a simple and fully-consistent picture of the cycling of rare earth elements (REEs) in the ocean as shown in Akagi (2013) has emerged.

1) Diatoms frustules over-supply REEs to the deep water.

2) The over-supplied REEs are removed from the deep water mainly by carbonate scavenging.

3) A part of REEs in deep water are incorporated in the form of silicic acid complex to diatom frustules in the surface water.

This picture is proved/endorsed by

I) consistency in the partitioning pattern between REEs scavenged by carbonate particles and those dissolved in seawater irrespective of sampling depths (Akagi, 2013),

II) the surface non-zero REE concentration explained by selective intake of REE silicic acid complexes by diatoms (Akagi, 2013),

III) mass balance between the over-supplied REEs and the scavenged REEs in the deep water (Akagi, 2013; Akagi et al., 2014), and

IV) identification of a new REE source to diatom frustules, which is supplied from the surface by upwelling or wind to compensate for those scavenged, attaining the steady state within a water column (Akagi et al., 2014).

Unfortunately the picture is incompatible with the conventional view on the REE circulation that has been constructed with diatom association being entirely neglected (Siddall, 2008; Rempfer, 2011; Oka, 2009; Arsouze, 2009). However, it is interesting to note that the two key features of the conventional view, i.e. the REE source of continental margin ("boundary exchange") and release of REEs from particles in the deep water ("reversible scavenge"), were also derived from the new picture where diatoms play a central role (Akagi et al., 2014). The presence of Al as much as 0.1% is also indicated in the course of the studies.

A series of these studies imply that other metals including trivalent Al might be taken in to diatom frustules together with REEs and that they may be transported to the deep water in a shape of silicate frustules or by being dissolved to the water medium together with frustule dissolution.

One of the reasons diatom frustules have not been considered as one of important carriers is difficulty in analyzing diatom frustules separately from terrigenous silicates. Some of earlier studies conclude that the contamination from clay cannot be entirely excluded even by meticulous separation of diatom opal (Shemesh et al, 1988; Ellwood et al, 1999; Andersen et al, 2011). In this study, estimation of the elemental composition of diatom frustules was carried out in the first time based on the aggregation-controlled dissolution kinetics of diatom frustules (Akagi et al., 2011) and the reasoning for the composition of diatom frustules was attempted by means of a box model analysis.

3.2. Methods

3.2.1. Sediment trap samples

Sediment trap samples were collected at Station AB (53°5'N, 177°W, water depth 3197 m) in the Aleutian Basin of the Bering Sea and Station SA (49°N, 174°W, water depth 5406 m) in the central subarctic Pacific (Fig. 3.1). To collect the samples a PARFLUX Mark 7G-13 time-series sediment trap with 13 rotary collections was deployed approximately 600 m above the seafloor.

Before the further analysis a sample was immersed in a storage solution to preserve the biogenic matter. The storage solution (5% formaldehyde solution) was prepared by mixing North Pacific deep seawater, formaldehyde and sodium borate buffer to adjust the pH from 7.6 to 8.0. Subsets of the samples were subjected to routine analysis for opal, calcium carbonate, and organic carbon contents, following the procedure described in Takahashi et al. (2002). Ten samples from Station AB and one sample from Station SA were analyzed for the elemental composition.

3.2.2. Compositional analysis

Settling particles separated from the formaldehyde storage solution by centrifugation were washed with 6 ml of ethanol and 3 ml of Milli-Q water, and freeze-dried. 10 mg of the dried sample (AB-20 #20: 4 mg) was treated with 10 ml of 40% acetic acid solution at 40°C for 25 minutes. After removing the solution, 10 ml of hydrochloric acid was added in the residue. The treatment with acetic acid and hydrochloric acid solutions is supposed to dissolve carbonates and oxides, respectively. The reason the samples were treated sequentially with different acids was to enable us to check the accuracy of the determination using an appropriate standard material. The solution of hydrochloric acid was removed and the residue, mainly consisting of siliceous matters was transferred to a Teflon vessel using 1 ml of nitric acid. Perchloric and hydrofluoric acids were added to the vessel and the residue was dissolved completely by heating for 90 minutes. After evaporation to dryness, HNO_3 solution and water were added and the final solutions (approx. 1 N HNO_3) were determined using inductivity coupled plasma mass spectrometry (ICP-MS; HP4500, Agilent Co., Ltd.). The accuracy of the whole analytical procedure was examined using standard rock material, JB-3, issued by Geological Survey of Japan and the errors of the sum of the three fractions are within 25% for Mg, Al, K, Ca, Sc, V, Cr, Mn, Fe, Co, Ni, Cu, Zn, Ga, Rb, Sr, Y, Zr, Nb, Mo, Cd, In, Ba, La, Ce, Pr, Nd, Sm, Eu, Gd, Tb, Dy, Ho, Er, Tm, Yb, Lu, Hf, Ta, W, Tl, Pb, Th, and U. The observed data was smaller than -50% for Li, Be, B, Na, and Sb; between -50% and -25% for Ti, I, and Cs; between 25% and 200% for Sn; greater than 200% for P and Ge. The compensate data of these elements were used for the discussion.

3.3. Results

3.3.1. Elemental composition of siliceous fraction and estimated composition of original diatom frustules

The measured values of elements in the siliceous fractions are converted to the concentration of diatom frustules on the basis of opal weight. Data of each element are shown in order of the periodic table in Fig. 3.2, where concentration data of each element are plotted against opal flux data. Most of elements exhibit a hyperbolic relationship against opal flux and approach to certain values when opal flux becomes greater (Li, Be, Na, Mg, Al, P, K, Ca, Sc, Ti, V, Cr, Mn, Fe, Co, Ni, Cu, Zn, Ga, Ge, Rb, Sr, Y, Zr, Nb, Mo, Ag, Sn, Sb, I, Cs, Ba, La, Ce, Pr, Nd, Sm, Eu, Gd, Tb, Dy, Ho, Er, Tm, Yb, Lu, Hf, Ta, W, Pb, Th, and U). One sample from SA (Opal flux = 82.05 mg m^{-2} day^{-1}) is plotted on the trend that the ten samples from AB form, and the sample was not treated separately. This consistency between the data from the two stations was reported earlier (Akagi et al., 2011). The hyperbolic relationship has already been reported for concentrations of rare earth elements (REEs) and aluminum in the different set of samples collected in 1995-1996 (Akagi et al., 2011; Akagi et al., 2013). The asymptotic values calculated as the average of five data whose opal flux is greater than 200 mg m^{-2} day^{-1} (AB-20#2, AB-20#3, AB-20#5, AB-20#9, AB-20#13) are listed in Table 3.1. The asymptotic values of REEs reported for the different set (Akagi, 2013) are also shown in Table 3.1. They are very similar to those of the present study for most of REEs. The data of B does not exhibit hyperbolic relationship. When the opal flux is small, the concentration values are typically 6 times as great as the asymptotic values. This relationship has been interpreted to be a result of selective dissolution of diatomaceous opal and/or attachment of terrigenous matter (Akagi et al., 2011). It should be noted that the asymptotic values are not zero, the implication of which will be discussed later.

3.4. Discussion

3.4.1. Determination of elemental composition in fresh diatomaceous frustules

According to Akagi et al. (2011), extent of chemical alternation of siliceous matter depends on degree of aggregation. In the course of development of the dissolution kinetics theory, the presence of "threshold value" has been discovered. Diatom frustules with a higher flux than the threshold value are considered to form mega-aggregates and they tend to settle down quickly through the column and to escape dissolution and/or alteration. On the other hand, frustules with a lower flux than the threshold value tend to be subjected to severe dissolution. In the case of REEs, the earlier studies (Akagi, 2013; Akagi et al., 2014) concluded the asymptotic composition should correspond to that of diatom frustules. The logic to conclude so, is summarized in Introduction part. The asymptotic values of REE and Al in the present study are very similar to those reported by the earlier study (Akagi, 2013) and we consider that the asymptotic values of other elements should correspond to the composition of diatom frustules. Another support for the discussion is the asymptotic Al/Si ratio of 0.0032 mol/mol, which is close to the slope of dissolved Al/Si (0.0022 mol/mol) seen in the Arctic Sea (Middag et al., 2009). In this study, in similar manner to Akagi (2013), the concentration data corresponding to the asymptotic values listed in Table 3.1 are adopted as the composition of diatom frustules in the Bering Sea.

We are aware of persistent criticism against our discussion, because the siliceous fraction we measured may have contained some of clay and radiolarian skeletons. However, non-zero asymptotic values indicate that the elements must be supplied somehow proportionally to opal amount up to infinite diatom production, which is difficult to explain if this were not the composition of diatom frustules. The next section also shows that the composition cannot be

explained simply by the contamination of clay.

3.4.2. Comparison of the composition of diatom silica frustules with that of the upper crust

Concentration ratios of each element against silicon (M/Si) in diatom frustules are compared to that of the upper crust (Rundnick et al., 2004) in Fig. 3.3. The composition ratio of diatom frustules for Ge and Sn (group 14 elements as the same as Si) is 1/5 and 2/5 of those of the upper crust respectively. REEs and other lithophile elements are contained at levels of 1/50-1/10 of the crust value. It seems that the difference in concentration among elements reflects their chemical properties. This will be discussed in section 4.3.

The plots are distributed in a rather narrow range: composition ratios (M/Si) of diatom frustules are in a ratio of 1-1/50 of those of upper crust. This shows an interesting contrast against biocarbonate minerals. In the case of coral, one of the most typical biogenic minerals, its composition ratios (M/Ca) (e.g. Bowen, 1979) distribute in a much wider range (1/1-1/10000) against the ratios of the upper crust. The narrow range (1/1-1/50) of Fig. 3.3 indicates the incorporation of terrigenous aluminosilicate, but at the same time, invalidates the idea of simple attachment of terrigenous silicates. One might interpret this distribution in terms of partial dissolution of terrigenous minerals, but if it is scrutinized closely, easier soluble elements like K is in a ratio similar to that of less soluble Al. Dissolution may not also explain why almost no element distributes below the 1/50 line.

Earlier studies (Akagi, 2013; Akagi et al., 2014) have identified two sources of REEs for diatoms: dissolved REEs in the form of silicic acid complexes in seawater and REEs in silicate minerals suspended in surface water. This intuitively explains the broad similarity and the dissimilarity in composition between diatom frustules and the upper crust, at the same time. Incorporation of the latter source is named “ocean weathering”, although the mechanism of

which remains unknown. In the "ocean weathering" almost no selection of REEs seems to be operative (Akagi et al., 2014). Regarding the former source, diatoms uptake silica through a specific channel, where a set of two specific proteins called "Q" captures silicic acid ions (Hildebrand, 2008) and this implicitly indicates that it cannot exclude silicic acid complexes where two apexes of silica tetrahedral remain intact. This may explains why diatoms uptake not only silicic acid but also silicate-metal complexes (Akagi, 2013).

3.4.3. A box model to express the concentration of elements in diatom frustules

Based on the recent discovery that diatoms incorporate both dissolved elements in the form of silicic acid complex and solid elements in silicate minerals, a box model has been worked out. Figures 3.4a and 3.4b illustrate the cycles of Si and terrigenous elements, in which diatoms are considered to play a dominant role in transportation within a water column. Because we discuss the concentration elements relative to that of Si, let us start with considering the cycle of Si, where diatoms have been established to play an almost exclusive role.

The production rate of diatoms, Si_{DF}, is expressed in terms of surface input rate of silicate minerals, Si_{AS}, and cycle rate of dissolved silica to diatom frustules in a column, Si_{D}.

$$Si_{\mathrm{DF}} = \varphi p Si_{\mathrm{AS}} + \psi_{\mathrm{Si}} Si_{\mathrm{D}}, \quad (1)$$

where φ denotes the dissolution proportion of silicates supplied to the surface of the column and p is the proportion taken in by diatoms and ψ_{Si} stands for the proportion of dissolved silica incorporated by diatoms (Fig. 3.4). Because diatoms play an almost exclusive role in the silica cycle, p and ψ_{Si} should be unity and omitted. Therefore,

$$Si_{\mathrm{DF}} = \varphi Si_{\mathrm{AS}} + Si_{\mathrm{D}}. \quad (2)$$

The generation rate of dissolved silica in a water column is controlled by the dissolution process of diatom frustules, i.e.,

$$Si_{\mathrm{D}} = f_{\mathrm{Si}} Si_{\mathrm{DF}}, \quad (3)$$

where f_{Si} is the proportion of dissolved diatom frustules. From eqs. (2) and (3), we obtain

$$Si_{\mathrm{DF}} = \frac{1}{1-f_{\mathrm{Si}}}\, \varphi Si_{\mathrm{AS}}. \quad (4)$$

In the same manner, circulation of terrigenous elements is considered (Fig. 3.4). The production rate of diatomaceous elements, M_{DF}, are expressed by

$$M_{\mathrm{DF}} = \varphi p M_{\mathrm{AS}} + \psi_{\mathrm{M}} M_{\mathrm{D}}. \quad (5)$$

In the case of general elements, ψ_{M} is the proportion of dissolved M in form of silicic acid complex (Akagi, 2013). The steady state condition for the flux of dissolved, M_{D}, leads to

$$M_{\mathrm{D}} = \varphi(1-p) M_{\mathrm{AS}} + f_{\mathrm{M}} M_{\mathrm{D}}. \quad (6)$$

By eliminating M_{D} from eqs. (5) and (6), we obtain

$$M_{\mathrm{DF}} = \frac{p+\psi(1-p)}{1-\psi f_{\mathrm{M}}} \varphi M_{\mathrm{AS}}. \quad (7)$$

Elemental composition in diatom frustules is expressed by the following equation dividing eq. (7) by eq. (4). i.e.,

$$\left(\frac{M}{Si}\right)_{\mathrm{DF}} = \frac{(1-f_{\mathrm{Si}})(p+\psi-\psi p)}{1-\psi f_{\mathrm{M}}} \left(\frac{M}{Si}\right)_{\mathrm{AS}}. \quad (8)$$

The siliceous fraction, SF, of sediment trap samples consists of mixture of undissolved alumino-silicate and undissolved silica-frustules, i.e.,

$$\left(\frac{M}{Si}\right)_{\mathrm{SF}} = \frac{(1-\varphi)M_{\mathrm{AS}} + (1-f)M_{\mathrm{DF}}}{(1-\varphi)Si_{\mathrm{AS}} + (1-f)Si_{\mathrm{DF}}} \quad (9)$$

$$= \left(1 - \frac{1-p-\psi-\psi f_{\mathrm{M}} + \psi p}{1-\psi f_{\mathrm{M}}} \varphi\right) \left(\frac{M}{Si}\right)_{\mathrm{AS}}. \quad (10)$$

When productivity of diatoms is infinitively great, M_{DF} is considered to be much greater than M_{AS}, i.e.,

$$(1-\varphi)M_{\mathrm{AS}} \ll (1-f_{\mathrm{M}})M_{DF} \quad (11)$$

and

$$(1-\varphi)Si_{\mathrm{AS}} \ll (1-f_{\mathrm{M}})Si_{DF} \quad . \tag{12}$$

Therefore, using eq. (11), (12) and (9)

$$\text{asymptotic } \left(\frac{M}{Si}\right)_{\mathrm{SF}} \approx \left(\frac{M}{Si}\right)_{\mathrm{DF}}. \tag{13}$$

The assumption of the box model is only valid to a group of terrigenous elements, such as Al, Ti, Ge and REEs, where their presence in the oceans is started with silicate matter supplied to the surface water. The diatom contribution in the cycle of REEs is well documented by some of our previous studies (Akagi, 2013; Akagi et al., 2014). Al, Ti and Ge are conventionally regarded as terrigenous elements. We considered that there may be other group of elements in circulation of which diatoms play a dominant role. We propose that Sc, Zr, Nb, Hf, Ta, W and REEs may be in this group, considering higher relative concentrations of these elements to Si (M/Si) in diatom frustules compared with the observed dissolved concentration increase relative to that of dissolved silica (ΔM/ΔSi) (Nozaki, 2001). The concentrations of Fe, Mn, Co, Mo, and Sn are also greater in diatom frustules than the observed concentration increase relative to dissolved silica, but the contribution of planktonic soft matter to their vertical transport may not be negligible in the five elements, because they are known as essential elements to plankton, and we did not apply them to the model.

For convenient sake, we introduce two simplifications to f_{si} and p. According to the recent compilation of the oceanic silica cycle (Tréguer, 2013), we set f_{si} to be 0.974, since 6.3 Tmol of the annual diatom production (240 Tmol) eventually is estimated to be removed to the seafloor per year. Our recent study of REEs cycles mediated by diatoms (Akagi et al., 2014) indicates that REEs in silicate minerals are incorporated to diatom frustules without significant fractionation, implying rather direct and unselective incorporation of elements in silicate minerals and we set p=1. Probably this may be oversimplification, but it will be shown that the simplification may be good enough for some elements.

Then we have

$$\left(\frac{M}{Si}\right)_{\mathrm{DF}} = \frac{0.026}{1-\psi f_{\mathrm{M}}}\left(\frac{M}{Si}\right)_{\mathrm{AS}}. \quad (14)$$

Let us examine how valid the equation is separately in the case of i) K, ii) REEs, iii) Al, and iv) other Sc, Zr, Nb, Hf, Ta, and W.

i) K

The silicic acid complex constants for monovalent ions are considered to be very small (Thakur, 2007) and the presence of silicic acid complex should be negligibly small. Because only metals in the form of silicic acid complex are supposed to be incorporated to diatom frustules (Akagi, 2013), ψ is set to zero. Therefore,

$$\left(\frac{\mathrm{K}}{\mathrm{Si}}\right)_{\mathrm{DF}} = 0.026\left(\frac{\mathrm{K}}{\mathrm{Si}}\right)_{\mathrm{AS}}. \quad (15)$$

The position of the plots for K is quite close to the relationship of eq. (15). The discrepancy between K and Na is due to much higher Na/K in seawater than Na/K in the upper crust.

ii) REEs

In the case of REEs the behavior is well documented by the leftover theory (Akagi, 2013). ψ is variable depending on REEs: ψ for La is 0.8, ψ for Nd is 0.85 and ψ for Lu is 0.9 approximately. Removal of REEs from the column is also calculated in the paper (Akagi, 2013), f_{La}, f_{Nd} and f_{Lu} are approximately 0.6, 0.5, and 0.9, respectively. Then we obtain

$$\left(\frac{\mathrm{La}}{\mathrm{Si}}\right)_{\mathrm{DF}} = 0.05\left(\frac{\mathrm{La}}{\mathrm{Si}}\right)_{\mathrm{AS}} \quad (16)$$

$$\left(\frac{\mathrm{Nd}}{\mathrm{Si}}\right)_{\mathrm{DF}} = 0.05\left(\frac{\mathrm{Nd}}{\mathrm{Si}}\right)_{\mathrm{AS}} \quad (17)$$

$$\left(\frac{\mathrm{Lu}}{\mathrm{Si}}\right)_{\mathrm{DF}} = 0.09\left(\frac{\mathrm{Lu}}{\mathrm{Si}}\right)_{\mathrm{AS}}. \quad (18)$$

The positions for the three elements look consistent with the consideration.

iii) Al

Aluminum is classified to scavenged element type in the Pacific Ocean, where vertical distribution decreases with depth increase. We cannot expect Al to be recycled to the surface in the North Pacific Ocean. *f* for Al is regarded as zero. Therefore,

$$\left(\frac{\mathrm{Al}}{\mathrm{Si}}\right)_{\mathrm{DF}} = 0.026\left(\frac{\mathrm{Al}}{\mathrm{Si}}\right)_{\mathrm{AS}}. \quad (19)$$

iv) Sc, Zr, Nb, Hf, Ta, and W

They show vertical profiles of nutrient type, where the concentration increases with depth increase. Therefore *f* should be greater than zero. But exact value estimation seems rather difficult due to the paucity of relevant supported data including vertical profies. Most of elements except Sc are tetravalent and their ψ values should be as great as 1. Therefore,

$$\left(\frac{\mathrm{M}}{\mathrm{Si}}\right)_{\mathrm{DF}} = \frac{0.026}{1-f_{\mathrm{M}}}\left(\frac{\mathrm{M}}{\mathrm{Si}}\right)_{\mathrm{AS}}. \quad (20)$$

The positions for M are always greater than 0.026 $(\mathrm{M/Si})_{\mathrm{AS}}$, and the exact positions may vary depending on *f* values.

The model seems to well explain the positions of some terrigenous elements in Figure 3.3.

Because, whatever element is, there must be at least one source of silicate mineral, the next equation should be valid.

$$\left(\frac{\mathrm{M}}{\mathrm{Si}}\right)_{\mathrm{DF}} > 0.026\left(\frac{\mathrm{M}}{\mathrm{Si}}\right)_{\mathrm{AS}}. \quad (21)$$

The aberration of the positions from the smallest $0.026(\mathrm{M/Si})_{\mathrm{AS}}$ should depend on the proportion of silicic complex, ψ_{M}, in the deep water (see Fig. 3.4). The vertical distribution of general recycled elements is controlled largely by the intake by plankton, and dissolution of organic matter in plankton. A part of those dissolved elements is in the form of silicic acid

complex, and this can be treated as extra input in the model and should explain the relationship of eq. (21).

3.5. Conclusion

The concentration of siliceous fraction of sediment trap samples collected in the North Pacific Ocean and the Bering Sea exhibited interesting asymptotic values when plotted against diatom fluxes. This hyperbolic relationship implies that the infinite diatom propagation would be sustained by the infinite supply of foreign elements. If all the elements in the diatom frustules are assumed to behave according to dissolution kinetics, similarly to rare earth elements, the asymptotic values should correspond to the original composition of the diatom frustules and we for the first time reported the compositional data of diatom frustules (see Introduction). The data seem to give some important implications in marine chemistry as listed below.

1) Diatom frustules are not pure opal but an impure substance, which contains elements at concentration as high as 1/10-1/50 that of terrigenous matter, relatively to silicon.

2) The high concentration of elements requires the extra supply of elements likely by the dissolution of silicate minerals suspending in the surface water.

3) Diatom frustules have a potential to supply many elements to the deep water by releasing the elements in the course of frustule dissolution.

The present study disclosed a hitherto-unexplored aspect of diatom frustules. The study is limited only to highly productive areas. Further studies in other areas of the oceans are necessary to generalize our discussion.

References

Akagi T., Fu F.-F., Hongo Y. and Takahashi K. (2011) Composition of rare earth elements in settling particles collected in the highly productive North Pacific Ocean and Bering Sea: implications for siliceous-matter dissolution kinetics and formation of two REE-enriched phases. *Geochim. Cosmochim. Acta* **75**, 4857-4876.

Akagi T. (2013) Rare earth element (REE)-silicic acid complexes in seawater to explain the incorporation of REEs in opal and the "leftover" REEs in surface water: New interpretation of dissolved REE distribution profiles. *Geochim. Cosmochim. Acta* **113**, 174-192.

Akagi T., Emoto M., Takada R. and Takahashi K. (2013) A diatom frustule is an impure entity: determination of biogenic aluminum and rare earth element composition in diatom opal and its implication for marine chemistry. In *Diatoms*. (ed. F. C. Bour). Nova Science Publishers, U. S. A.

Akagi T., Yasuda S., Asahara Y., Emoto M. and Takahashi K. (2014) Diatoms spread a high ε_{Nd}-signature in the North Pacific Ocean. *Geochem. J.* **48**, 121-131.

Andersen M. B., Vance D., Archer C., Anderson R. F., Ellwood M. J. and Allen C. S. (2011) The Zn abundance and isotopic composition of diatom frustules, a proxy for Zn availability in ocean surface seawater. *Earth Planet. Sci. Lett.* **301**, 137-145.

Arsouze T., Dutay J.-C., Lacan F. and Jeandel C. (2009) Reconstructing the Nd oceanic cycle using a coupled dynamical-biogeochemical model. *Biogeosci. Discuss.* **6**, 5549-5588.

Bowen H. J. M. (1979) Environmental chemistry of the elements. Academic Press, pp. 99-101.

de la Rocha C. L., (2006) The biological pump. In *The Ocean and Marine Geochemistry. Treatise on Geochemistry*, vol. 6 (ed. H. Elderfield). Elsevier-Pergamon, Oxford.

Ellwood M. J. and Hunter K. A. (1999) Determination of the Zn/Si ratio in diatom opal: a

method for the separation, cleaning and dissolution of diatoms. *Mar. Chem.* **66**, 149-160.

Hildebrand M. (2008) Diatoms, biomineralization processes, and genomics. *Chem. Rev.* **108**, 4855-4874.

Middag, R., de Baar, H. J. W. Laan, P. and Bakker, K. (2009) Dissolved aluminium and the silicon cycle in the Arctic Ocean. *Mar. Chem.* **115**, 176-195.

Nozaki, Y. (2001) Elemental distribution. In *Encyclopedia of Ocean Sciences*, vol. 2 (eds. J. H. Steel et al.). Academic Press, pp. 840-845.

Oka A., Hasumi H., Obata H., Gamo T. and Yamanaka Y. (2009) Study on vertical profiles of rare earth elements by using an ocean general circulation model. *Global Biogeochem. Cycles* **23**, GB4025, doi:10.1029/2008GB003353.

Rempfer J., Stocker T. F., Joos F., Dutay J.-C. and Siddall M. (2011) Modelling Nd-isotopes with a coarse resolution ocean circulation model: Sensitivities to model parameters and source/sink distributions. *Geochim. Cosmochim. Acta* **75**, 5927-5950.

Rudnick R. L. and Gao S. (2004) Composition of the continental crust. In *The Crust. Treatise on Geochemistry*, vol. 3 (ed. R. L. Rudnick). Elsevier-Pergamon, Oxford.

Shemesh A., Mortlock R. A., Smith R. J. and Froelich P. N. (1988) Determination of Ge/Si in marine siliceous microfossils: separation, cleaning and dissolution of diatoms and radiolarian. *Mar. Chem.* **25**, 305-323.

Siddall M., Khatiwala S., van de Flierdt T., Jones K., Goldstein S. L., Hemming S. and Anderson R. F. (2008) Towards explaining the Nd paradox using reversible scavenging in an ocean general circulation model. *Earth Planet. Sci. Lett.* **274**, 448-461.

Takahashi K., Fujitani N. and Yanada M. (2002) Long term monitoring of particle fluxes in the Bering Sea and the central subarctic Pacific Ocean, 1990-2000. *Progr. Oceanogr.* **55**, 95-112.

Tréguer P. (2013) The world ocean silica cycle. *Annual review of marine science* **5**, 477-501.

Thakur P., Singh D. K. and Choppin G. R. (2007) Polymerization study of o–$Si(OH)_4$ and complexation with Am(III), Eu(III) and Cm(III). *Inorg. Chim. Acta* **360**, 3705-3711.

Table 3.1 Concentration (μg/g) of diatom frustules estimated from the asymptotic values in Figure 1
a) Reported values of Akagi (2013) are noted in the parentheses
b) Concentration (μg/g) of the upper crust (Rundnick et al., 2004)
c) $SiO_2 \cdot nH_2O$ theoretical value

element	Diatom frustules [a)]	D.L.	Upper crust [b)]	element	Diatom frustules [a)]	D.L.	Upper crust [b)]
Li	8.9	0.033	21	Ag	0.12	0.00068	0.053
Be	0.21	0.00028	2.1	Sn	1.1	0.024	2.1
Na	11000	30	28300	Sb	2.1	0.018	0.4
Mg	3200	0.093	15000	I	5.0	0.26	1.4
Al	9000 (1600)	0.54	81500	Cs	0.52	0.00030	4.9
Si	417400 [c)]	-	311400	Ba	460	0.16	624
K	1500	52	23200	La	1.3 (1.20)	0.00058	31
Ca	3300	23	20000	Ce	2.8 (2.3)	0.00030	63
Sc	1.9	0.026	14.0	Pr	0.35 (0.28)	0.00029	7.1
Ti	510	0.26	3800	Nd	1.0 (1.04)	0.00051	27
V	16	0.011	97	Sm	0.34 (0.23)	0.00058	4.7
Cr	5.8	0.12	92	Eu	0.15 (0.057)	0.00030	1.0
Mn	110	0.18	770	Gd	0.32 (0.24)	0.00029	4.0
Fe	5600	18	39200	Tb	0.052 (0.038)	0.00030	0.7
Co	2.0	0.0011	17.3	Dy	0.30 (0.24)	0.00033	3.9
Ni	2.5	0.0063	47	Ho	0.068 (0.051)	0.00035	0.83
Cu	20	0.019	28	Er	0.19 (0.17)	0.00042	2.3
Zn	39	0.12	67	Tm	0.030 (0.025)	0.00047	0.30
Ga	2.9	0.0018	17.5	Yb	0.23 (0.18)	0.00058	2.0
Ge	0.29	0.00351	1.4	Lu	0.034 (0.029)	0.00032	0.31
Rb	5.1	0.0017	84	Hf	0.45	0.0020	5.3
Sr	55	0.0093	320	Ta	0.049	0.00009	0.9
Y	1.7	0.00079	21	W	0.24	-	1.9
Zr	20	0.056	193	Pb	2.8	0.018	17
Nb	0.66	0.0073	12	Th	0.62	0.00045	10.5
Mo	0.24	0.019	1.1	U	0.43	0.00009	2.7

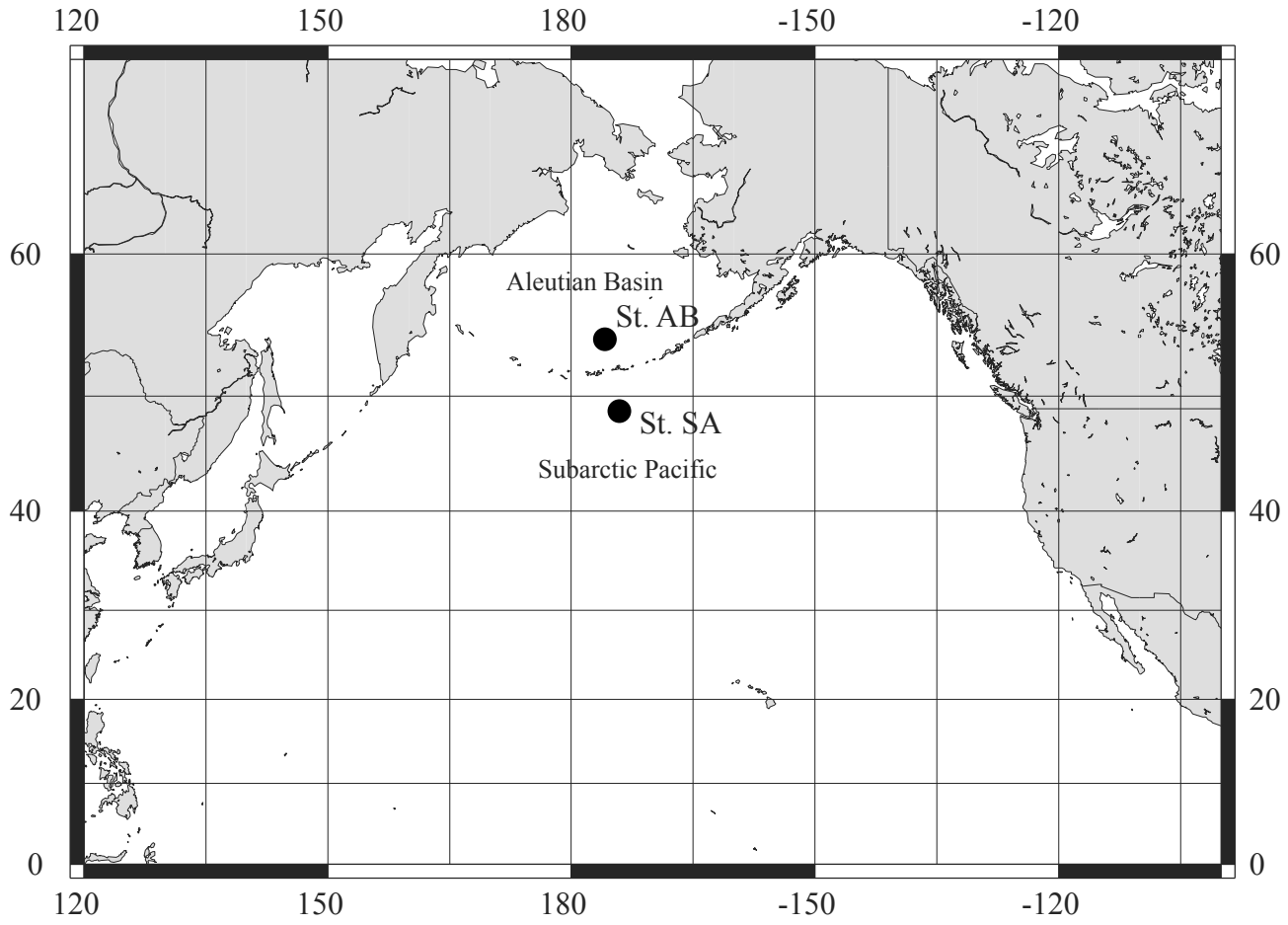

Fig. 3.1 Map showing the location of studied sites: Station AB (53.5°N, 177°W) and Station SA (49°N, 174°W).

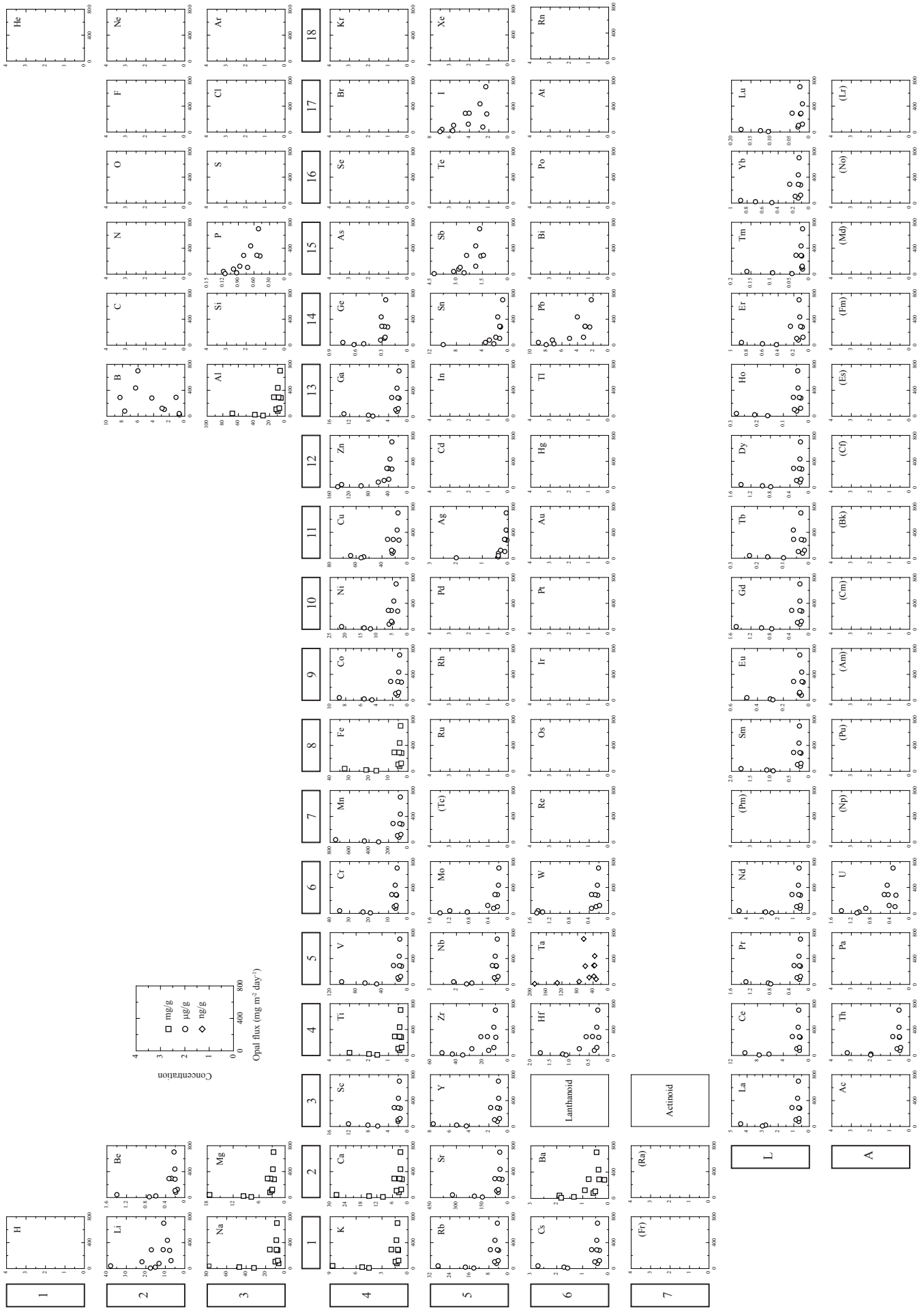

Fig. 3.2 Concentrations of elements in siliceous fractions plotted against opal flux in an order of periodic table. The elements whose concentrations are close to the lower detection limits are not shown.

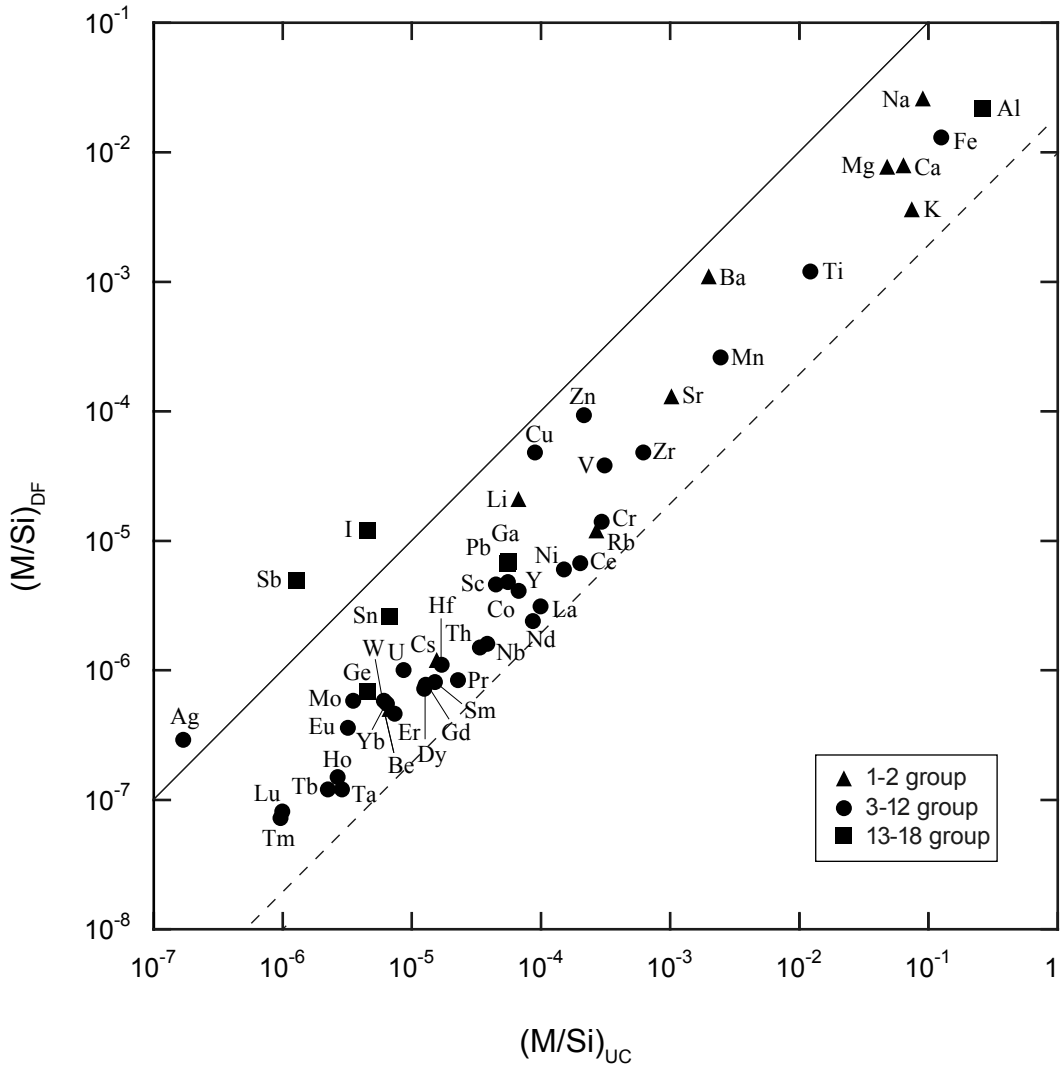

Fig. 3.3 M/Si in diatom frustules vs M/Si in the upper crust. The solid line shows 1:1 relationship and dotted line 1:50 relationship.

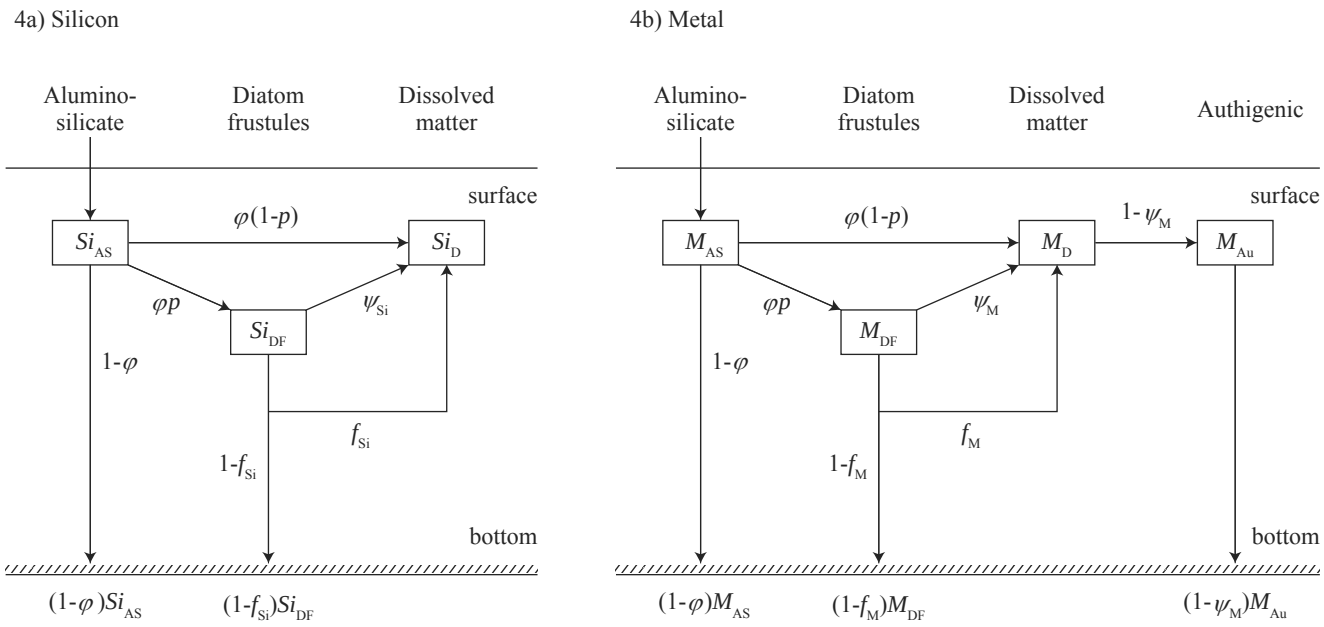

Fig. 4 Box model structures of silicon (a) and terrigenous elements (b). See text for details.

Chapter 4

Al-NMR studies of the settling particles collected in the highly diatom-productive Bering Sea: a new evidence for silicate dissolution/incorporation by diatoms

4.1. Introduction

Our recent studies of rare earth elements (REEs) in the settling particles from the highly diatom productive Bering Sea have led to a novel picture of the oceanic cycle of REEs (Akagi, 2013; Akagi et al., 2013; Akagi et al., 2011; Akagi et al., 2014): Diatom frustules are main carriers of REEs in a water column and the REEs in diatom frustules are released to seawater in the course of dissolution of the frustules. The concentrations of REEs in diatom frustules are higher by a factor of about 2 (LREEs and MREEs) or by a factor of about 1.1 (HREEs) than their concentration increase relative to silicic acid concentration increase. This discovery further has led to the identification of carbonate as a REE scavenger from the surface of the water column (Akagi et al., 2014). In other words REEs in silicate minerals should somehow be taken in by diatoms: probably through dissolution of silicate minerals by diatoms. This novel diatom involvement with the oceanic REE cycle deeply challenges the conventional explanation of REE distribution in terms of "reversible scavenging" (Oka et al., 2009; Siddall et al., 2008) and "boundary exchange" (Arsouze et al., 2009; Rempfer et al., 2011). Further evidence of diatom association of silicate dissolution is prerequisite.

Aluminum is one of the most typical terrigenous metals like REEs. If diatoms really dissolve silicate minerals and take in REEs, it is likely that Al is also present in diatom frustules in

different states from those in clay and silicate minerals. The concentration of Al in diatom frustules is of 0.1% level and Al/Si ratio (mol/mol) range between 7×10^{-5} and 8×10^{-3}, with an average value of 5×10^{-3} (Gehlen et al., 2002; Akagi et al., 2013; Akagi et al., 2011), which is much higher than the ratio of Al/Si dissolved in the Pacific Ocean water (10^{-5}-10^{-6}; Orians and Bruland, 1986). When the concentrations of REEs and Al in siliceous fraction of sediment trap samples are plotted against opal flux, they show a hyperbolic relationship with non-zero asymptotic values, seemingly implying that infinite diatom productivity requires infinite supply of terrigenous elements. The concentrations of REEs and Al in diatom frustules were determined as the asymptotic value of siliceous fraction in sediment trap samples (Akagi et al., 2013; Akagi et al., 2011). Regardless of opal flux, the majority of Al (80%) was present in siliceous fraction, which cannot be leached by hydrochloric acid (Akagi et al., 2013; Akagi et al., 2011). If Al is present in the sediment trap samples of an opal flux, high enough to give the asymptotic value, in states other than clay or silicate minerals, this may provide supportive evidence of the presence of indigenous Al in diatoms. In this study the chemical state of Al in siliceous fraction of sediment trap samples has been investigated using nuclear magnetic resonance (NMR) spectroscopy.

4.2. Methods

4.2.1. Sediment trap samples

The Bering Sea is extremely high productivity region and diatoms are major contributor of biogenic silica (Takahashi et al., 2002). Sediment trap samples were collected at Station AB (53°5'N, 177°W, water depth 3197 m) in the Aleutian Basin of the Bering Sea (Fig. 4.1). To collect the samples a PARFLUX Mark 7G-13 time-series sediment trap with 13 rotary

collections was deployed approximately 600 m above the seafloor.

Before further analysis a sample was immersed in a storage solution to preserve the biogenic matter. The storage solution (5% formaldehyde solution) was prepared by mixing North Pacific deep seawater, formaldehyde and sodium borate buffer to adjust the pH from 7.6 to 8.0. Subsets of the samples were subjected to routine analysis for opal, calcium carbonate, and organic carbon contents, following the procedure described in Takahashi et al. (2002). As for opal analysis, opal was leached by 0.5 M Na_2CO_3 solution at 80°C for 5 h after pretreatment of 10% hydrogen peroxide solution and 1 N HCl solution for removing organic matter and carbonate. Si concentration of the solutions was measured employing molybdenum yellow method and converted into opal contents.

We chose five samples, which vary in productivity, from a series of samples collected in 2008 for measurement of NMR, X-ray diffractometer (XRD), and inductivity coupled plasma-optical emission spectrometer (ICP-OES).

4.2.2. NMR spectroscopy

The ^{27}Al MAS NMR spectra were recorded on a JEOL ECA 400 spectrometer operating at a resonance frequency of 104.2 MHz. The samples collected from the slide glass after XRD measurements were packed into ZrO_2 rotors and spun at 12 kHz. The signals were integrated over 11,000-340,000 scans with a delay time of 0.8 s. ^{27}Al chemical shift was reported in ppm relative to the signal for $[Al(H_2O)_6]^{3+}$ used as an external standard.

4.2.3. XRD spectrum

Settling particles separated from the formaldehyde storage solution by centrifugation were washed with 6 ml of ethanol and 3 ml of Milli-Q water. A portion of a washed sample was

thinly pasted on a slide-glass and dried at room temperature prior to XRD (Mac Science, M18XHF22). XRD spectrums were obtained using CuKα radiation at 40 kV and 50 mA with; steps of 0.05° and a counting time of 4 s at each step.

4.2.4. ICP-OES

A part of washed sample was freeze-dried for determination of Al composition. Typically 10 mg of a dried sample (4 mg for AB-20 #20) was treated with 10 ml of 40% acetic acid solution at 40°C for 25 minutes. A supernatant solution was separated from residue (HAc residue) by centrifugation. After the supernatant solution was evaporated to dryness, HNO_3 solution and water were added to prepare a final solution (HAc fraction) for ICP-OES measurement. 10 ml of hydrochloric acid was added to the HAc residue. The solution was separated by centrifugation and evaporated and then HNO_3 solution and water were added to make a final solution (HCl fraction). The treatment with acetic acid and 3% hydrochloric acid solutions is supposed to dissolve carbonates and oxides, respectively. The HCl residue, mainly consisting of siliceous matters, was transferred to a Teflon vessel using 1 ml of nitric acid. 1 g of 70% perchloric and 1 g of 35% hydrofluoric acids were added to the vessel and the residue was decomposed completely by heating for 90 minutes. After evaporation, HNO_3 solution and water were added and the final solution was named HF fraction. The Al concentration of the three final solutions (approx. 1 N HNO_3) was determined using ICP-OES (Agilent 5100). The Al composition of settling particles was calculated as summation of Al amounts of the HAc, HCl, and HF fractions.

4.3. Results & Discussion

4.3.1. ^{27}Al MAS NMR spectra of sediment trap samples

Fig. 4.2 shows the ^{27}Al MAS NMR spectra for the sediment trap samples. The NMR spectra of all five samples show two peaks: one around 0-10 ppm and the other around 60-70 ppm. The spectra could be de-convoluted into minimum number of three peaks with reasonably small residues: typically two broad peaks at 70 ppm (line 1) and 0 ppm (line 4), and a sharp peak at 60 ppm (line 2) (Fig. 4.2, Table 4.1). In the case of sample AB-20#17, the broad peak at 70 ppm (line 1) is missing and a new peak (line 3) was observed at 40 ppm (Fig. 4.2).

^{27}Al NMR spectra yield information on the coordination number of aluminum ions based on chemical shift (in ppm): The chemical shift ranges from -10 to 30 ppm for 6-coordinated aluminum (AlO_6, Al(6)), from 30 to 40 ppm for 5-coordinated aluminum (AlO_5, Al(5)) and from 40 to 80 ppm for 4-coordinated aluminum (AlO_4, Al(4)) (Engelhaldt and Michel, 1987; Isobe et al., 2003). The two broad peaks around 70 ppm and 0 ppm (lines 1 and 4) can be attributed to Al(4) and Al(6), respectively. The sharp peak (line 2) is located at approximately 10 ppm smaller than that of the broad peak of Al(4). We attributed the sharp peak to Al(4) in well-structured silicate minerals, and the broad peak at 70 ppm to Al(4) in poorly-structured forms such as amorphous silica. The peak (line 3) observed only in sample AB-20#17 may be due to Al(5) based on its chemical shift (Engelhaldt and Michel, 1987).

Machill et al. (2013) cultivated diatoms with media doped with $AlCl_3$ and observed two broad peaks in ^{27}Al MAS NMR spectra and attributed them to Al(4) and Al(6). They reported three spectra and interestingly two of their NMR spectra are almost identical to those observed in this study: one spectrum to those of AB-20#2, #11, #13 and #20; one to that of exceptional AB-20#17. Gehlen et al. (2002) concluded that only Al(4) was present in cultured diatoms

based on the study of Al K-edge XANES and EXAFS spectra. They reported Al of Al(4) and Al(6) states in natural diatom samples, but they considered that the Al(6) was possibly due to contamination of clay mineral. The presence of the broad Al(6) (line 4) in the cultivated diatoms (Machill et al., 2013) imply that the Al(6) in natural diatom samples is not necessarily due to contamination of clay minerals. We will discuss this possibility further.

4.3.2. Variation of line intensities in spectra and its interpretation

In sediment trap samples more than 80% of Al is present in a siliceous fraction with the rest being soluble in acetic and hydrochloric acid (Table 4.2). A part of Al(6) can be attributed to not only clay minerals but also amorphous $Al(OH)_3$ or gibbsite in the case of the present samples. However, gibbsite was not detected by XRD measurements (Fig. 4.3). Isobe et al. (2003) investigated the coordination numbers of amorphous $Al(OH)_3$ and gibbsite based on ^{27}Al MAS NMR spectra. Although small peaks corresponding to Al(4) and Al(5) were observed in amorphous $Al(OH)_3$, sharp Al(6) is dominant line in both the substances. We concluded that the amounts of amorphous $Al(OH)_3$ and gibbsite are negligibly small in any of our samples.

Most of samples have reside/(opal+residue) ratios as small as 0.2, but sample AB-20#17 has an exceptionally high residue/(opal+residue) ratio greater than 0.4. It is suggested that the missing of line 1, intensified line 2 and emergence of line 3 for the sample are due to presence of exceptional aluminosilicate. The specificity of AB-20#17 is supported by its XRD spectrum with significant amounts of plagioclase, quartz and chlorite (Fig. 4.3).

Al(4) and Al(6) in clay minerals normally appear as sharper peaks (Sanz and Serratosa, 1984; Woessner, 1989) than those observed in this study. However, it is interesting to note that Al(5) has never been reported for natural clay minerals. In the case of our samples, the intensity ratio of sharp line 2/broad line 4 seems to correlate with residue/(opal+residue) ratios (r^2=0.83,

P=0.03). Therefore, sharp line2 may be due to Al in clay minerals. This is supported by the XRD spectra of samples, where the peaks of clay minerals were intensified with increasing order of line2/line4 ratios. The scrutiny of the spectra identifies a noisy projection at the apex of line 4 in most samples. This is likely due to the presence of clay minerals at relatively small amount.

4.3.3. Implication for presence of authigenic Al in diatom frustules

Akagi et al. (2011) developed the aggregation-controlled dissolution kinetics of diatom frustules, and explained the variations of concentration of rare earth elements in siliceous matter of sediment trap samples in terms of selective dissolution of opal from aggregated diatom frustules. Briefly, the dissolution of diatom frustules is largely governed by their aggregation. When the productivity is infinite, the dissolution rate of aggregates is negligibly small as a result of infinitely large size of the aggregates. The concentration of elements in the aggregated frustules should be an original (or unaltered) value when diatom productivity is infinitely great. They also observed that the composition of siliceous matter collected at Station AB in the Bering Sea at productivity >200 mg m^{-2} day^{-1} was almost constant and that it could represent that of the diatom frustules inexperienced with dissolution. The present five samples are consistent with this rule, and the Al concentration of the five samples show a hyperbolic relationship against opal flux with a non-zero asymptotic value (Fig. 4.4a). Compared with Al, amorphous silica is more soluble (Dixit et al., 2001). Normally this hyperbolic relationship is interpreted by mixing with diatom frustules and clay minerals. The reason that they employed the dissolution kinetic instead of mixing is presence of positive Ce anomaly when opal flux is small, which cannot be understood by the mixing of diatoms and clay (Akagi et al., 2011). Except for exceptional sample AB-20#17, the Al concentration does not show a good

correlation with the relative intensity of sharp line 2 (Fig. 4.4b). The similarity of the Al-NMR spectra of the sample with the greatest productivity (Sample AB-20#2, opal flux = 439 mg m^{-2} day^{-1}) to that with the smallest one (Sample AB-20#20, opal flux = 10 mg m^{-2} day^{-1}) (Fig. 4.2) seems to imply that most of Al in the siliceous fraction of settling particles is in similar states in diatom frustules, at any diatom productivity, simply with different levels of opal dissolution depending on diatom productivity. This is supportive of the dissolution kinetics, but is incompatible with the idea of mixing with clay. The concentration of Al is higher accordingly with decreasing opal flux (Fig. 4.4a). Even when Al concentration is high, the major broad NMR peaks of Al simply indicate that most of Al is not from clay, but from that in diatom frustules.

4.3.4. Support for diatomaceous dissolution/incorporation of metals in silicate minerals

In the Bering Sea the Al concentration in siliceous fraction decreases down to 0.1% at extremely high opal flux of more than 200 mg m^{-2} day^{-1} (Akagi et al., 2011). This concentration is smaller than the Al concentration of the present sediment trap samples of highest flux and the most of Al is in siliceous fraction. The NMR spectra in this study imply that this Al exists in diatom frustules in different states from those in clay or silicate minerals. The Al/Si ratios of the diatom frustules are more than 10^3 times higher than that dissolved in Pacific deep water (Orians and Bruland, 1986). This level of Al concentration cannot be explained without addition of Al in the surface water. Again the present study invalidates the idea of simple admixing of clay minerals. The results may be explained only by the newly discovered physiological action of diatom dissolution/incorporation of silicate minerals (Akagi et al., 2014).

4.4. Conclusion

Broad peaks of NMR spectra of Al in the sediment trap samples collected from the diatom-dominated Bering Sea is distinct from those of Al in clay and silicate minerals. The sharp peak of Al(4) was observed, but it is relatively weak. Importantly the spectra are similar to each other irrespective of opal flux, a measure of diatom productivity, and irrespective of Al amount, and also are similar to the reported spectra obtained by Al ion-doped diatom cultivation study (Machill et al., 2013). In the samples 80% of Al is in siliceous fraction. Therefore the chemical states of most of Al in the samples are concluded to be distinct from those of usual silicate minerals such as clay or silicate minerals and to be due to Al indigenous to diatom frustules. The geochemical implication is that Al cannot be taken as a proxy of aluminosilicate. To explain this amount of high Al concentration in diatom frustules, an extra supply of Al from silicate minerals to the photic seawater zone is necessary, which is supportive of the recent discovery of extra input of REEs to diatoms in the surface water.

References

Akagi, T. (2013) Rare earth element (REE)–silicic acid complexes in seawater to explain the incorporation of REEs in opal and the "leftover" REEs in surface water: New interpretation of dissolved REE distribution profiles. *Geochim. Cosmochim. Acta* **113**, 174-192.

Akagi, T., Emoto, M., Tadkada, R. and Takahashi, K. (2013) Diatom frustule is an impure entity: Determination of biogenic aluminum and rare earth element composition in diatom opal and its implication on marine chemistry, in *Distoms - Diversity and Distribution, Role in Biotechnology and Environmental Impacts,* **127**, p.1-34, Nova Science Publishers, Inc.,

New York.

Akagi, T., Fu, F.-f., Hongo, Y. and Takahashi, K. (2011) Composition of rare earth elements in settling particles collected in the highly productive North Pacific Ocean and Bering Sea: Implications for siliceous-matter dissolution kinetics and formation of two REE-enriched phases. *Geochim. Cosmochim. Acta* **75**, 4857-4876.

Akagi, T., Yasuda, S., Asahara, Y., Emoto, M. and Takahashi, K. (2014) Diatoms spread a high ε_{Nd}-signature in the North Pacific Ocean. *Geochem. J.* **48**, 121-131.

Arsouze, T., Dutay, J.-C., Lacan, F. and Jeandel, C. (2009) Reconstructing the Nd oceanic cycle using a coupled dynamical-biogeochemical model. *Biogeosciences* 6, 5549-5588.

Engelhaldt, G. and Michel, D. (1987) High Resolution Solid State NMR of Silicates and Zeolites, John Wiley & Sons, New York.

Dixit, S., Van Cappellen, P. and van Bennekom, A. J. (2001) Processes controlling solubility of biogenic silica and pore water build-up of silicic acid in marine sediments. *Mar. Chem.* **73** 333-352.

Gehlen, M., Beck, L., Calas, G., Flank, A.-M., Van Bennekom, A. J. and Van Beusekom, J. E. E. (2002) Unraveling the atomic structure of biogenic silica: Evidence of the structural association of Al and Si in diatom frustules. *Geochim. Cosmochim. Acta* **66**, 1601-1609.

Isobe, T., Watanabe, T., d'Espinose de la Caillerie, J. B., Legrand, A. P. and Massiot, D. (2003) Solid-state ^{1}H and ^{27}Al NMR studies of amorphous aluminum hydroxides. *J. Colloid Interface Sci.* **261**, 320-324.

Machill, S., Köhler, L., Ueberlein, S., Hedrich, R., Kunaschk, M., Paasch, S., Schulze, R. and Brunner, E. (2013) Analytical studies on the incorporation of aluminium in the cell walls of the marine diatom *Stephanopyxis turris*. *Biometals* **26**, 141-150.

Oka, A., Hasumi, H., Obata, H., Gamo, T. and Yamanaka, Y. (2009) Study on vertical profiles of

rare earth elements by using an ocean general circulation model. *Global Biogeochem. Cycles* **23**, GB4025, doi:10.1029/2008GB003353.

Orians, K. J. and Bruland, K. W. (1986) The biogeochemistry of aluminum in the Pacific Ocean. *Earth Planet. Sci. Lett.* **78**, 397-410.

Rempfer, J., Stocker, T.F., Joos, F., Dutay, J.-C. and Siddall, M. (2011) Modelling Nd-isotopes with a coarse resolution ocean circulation model: Sensitivities to model parameters and source/sink distributions. *Geochim. Cosmochim. Acta* **75**, 5927-5950.

Sanz, J. and Serratosa, J. M. (1984) ^{29}Si and ^{27}Al High-Resolution MAS-NMR Spectra of Phyllosilicates. *J. Am. Chem. Soc.* **106**, 4790-4793.

Siddall, M., Khatiwala, S., van de Flierdt, T., Jones, K., Goldstein, S.L., Hemming, S. and Anderson, R.F. (2008) Towards explaining the Nd paradox using reversible scavenging in an ocean general circulation model. *Earth Planet. Sci. Lett.* **274**, 448-461.

Takahashi K., Fujitani N. and Yanada M. (2002) Long term monitoring of particle fluxes in the Bering Sea and the central subarctic Pacific Ocean, 1990-2000. *Progr. Oceanogr.* **55**, 95-112.

Woessner, D. E. (1989) Characterization of clay minerals by ^{27}Al nuclear magnetic resonance spectroscopy. *American Mineralogist* **74**, 203-215.

Table 4.1 Peaks observed in ^{27}Al MAS NMR spectra of sediment trap samples.

Sample	Chemical shift (ppm)				Area ratio (%)			
	Line 1	Line 2	Line 3	Line 4	Line 1	Line 2	Line 3	Line 4
AB-20#2	66.6	60.9		0.0	39	2		59
AB-20#11	72.0	60.8		5.74	30	4		66
AB-20#13	65.4	61.6		0.036	57	9.2		33
AB-20#17		53.0	37.4	-4.68		28.7	27.6	43.7
AB-20#20	70.4	60.0		3.64	33	3		64

Table 4.2 Al concentration, opal flux and residual ratio for sediment trap samples.

Sample	Al concentration	Al (%) in fraction			Opal flux	residue/(opal+residue)
	(μg/g)	HAc	HCl	HF	(mg m^{-2} day^{-1})	
AB-20#2	7100	3.3	6.8	89.9	438.9	0.20
AB-20#11	4700	5.0	6.1	88.9	126.1	0.19
AB-20#13	9700	4.8	4.7	90.5	294.3	0.22
AB-20#17	32000	3.0	3.6	93.5	45.1	0.44
AB-20#20	19000	6.4	6.9	86.7	0.5	-

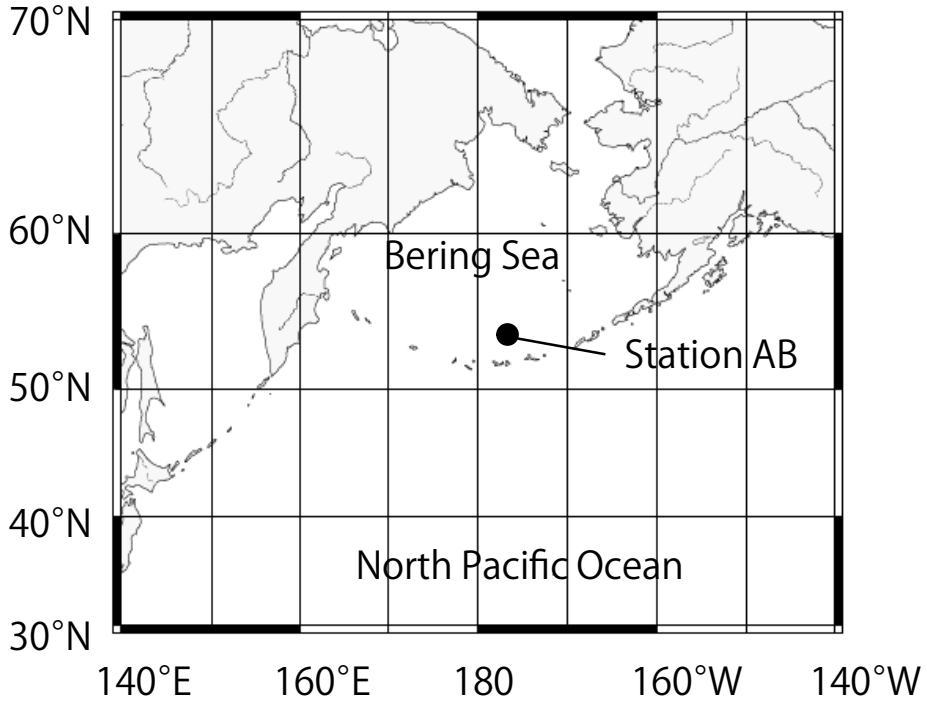

Fig. 4.1 Map shows the location of studied sites: Station AB (53°5’N, 177°W, water depth 3197 m).

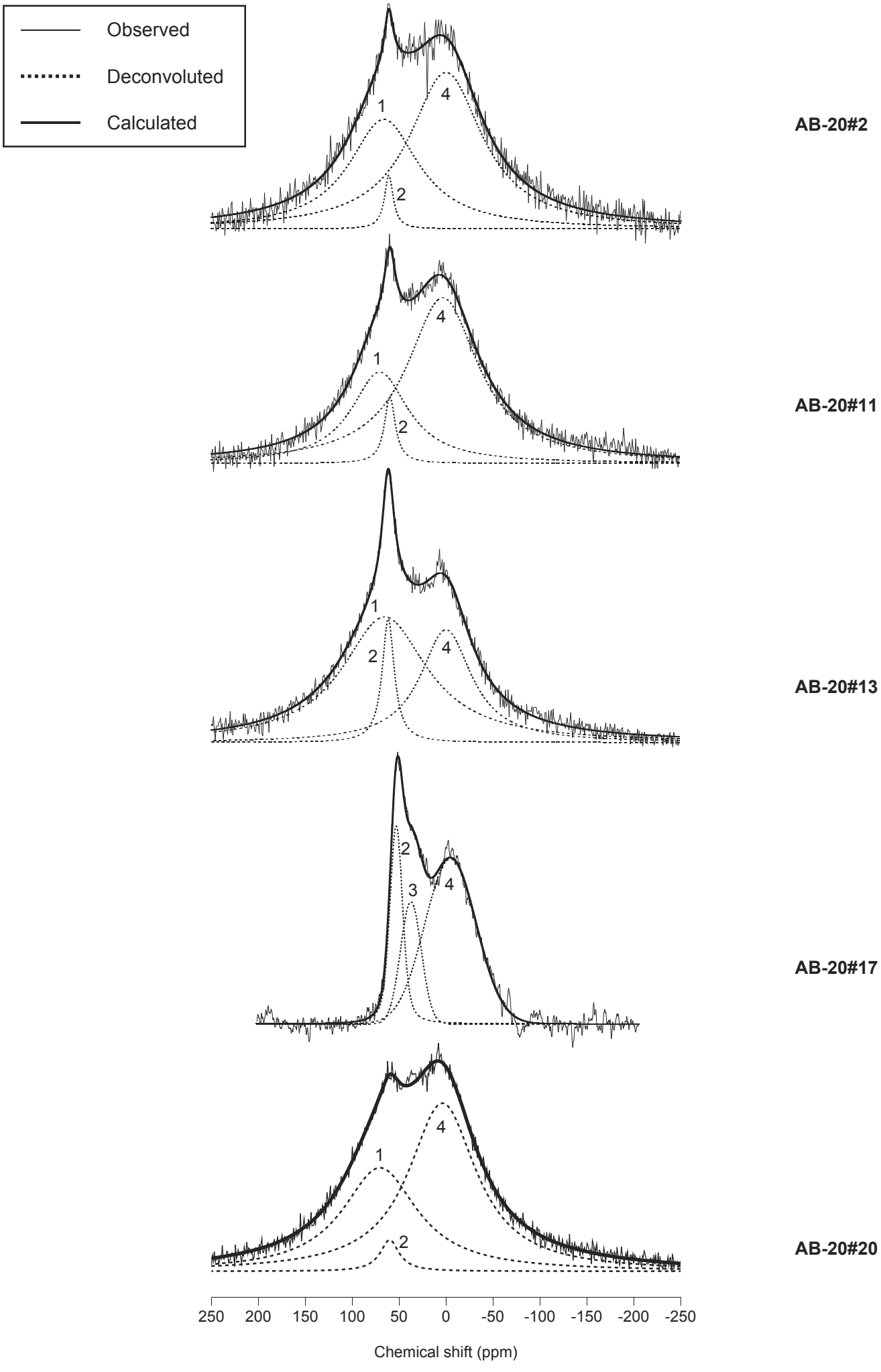

Fig. 4.2 ^{27}Al MAS NMR spectra of the sediment trap samples and de-convoluted lines.

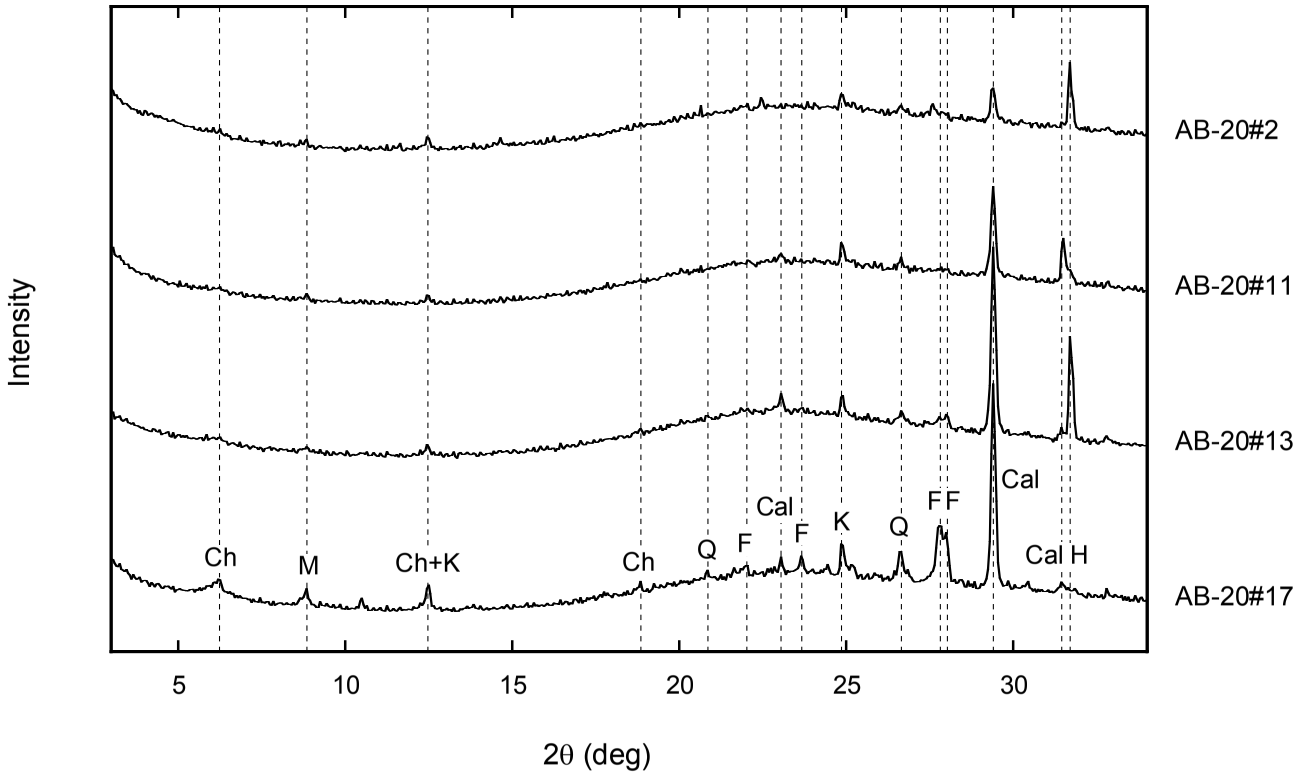

Fig. 4.3 XRD patterns of settling particles. Q, quartz; Cal, calcite; M, muscovite; K, kaolinite; Ch, chlorite; F, feldspar; H, halite.

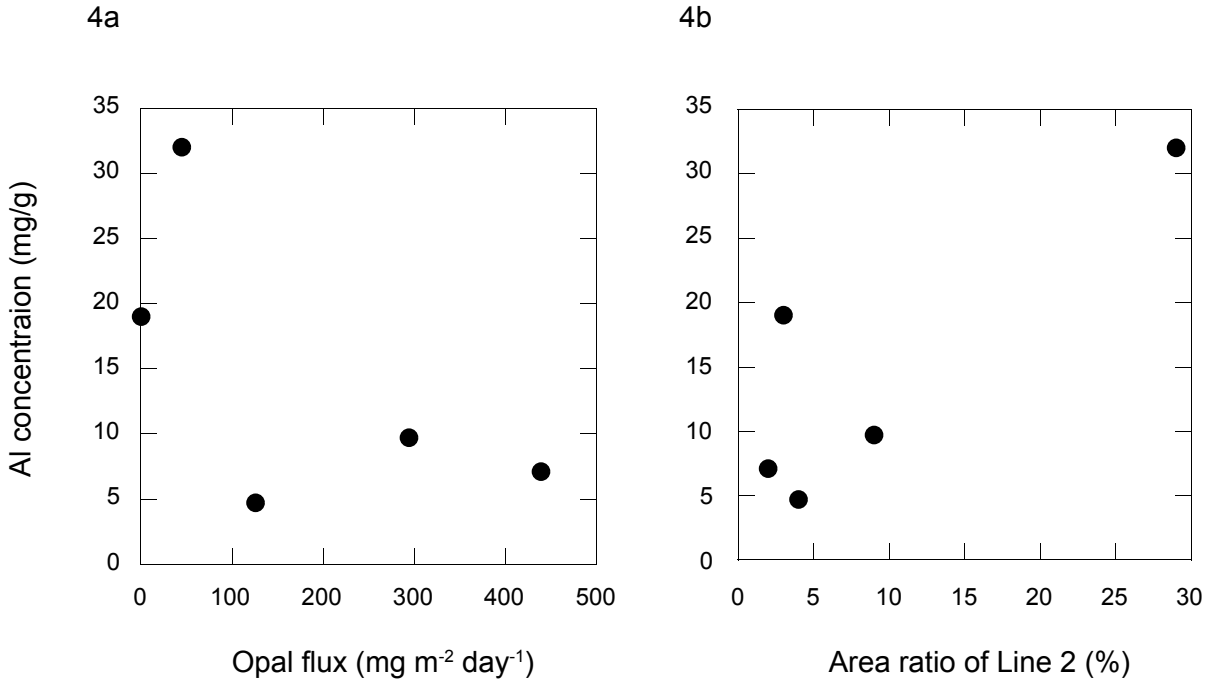

Fig. 4.4a Al concentration in settling particles at various opal flux.
Fig. 4.4b Relation of Al concentration in settling particles and area ratio of sharp peak (line 2).

Chapter 5

Problems on the chemical analyses of diatom frustules

5.1. Introduction

Chapters 3 and 4 show that diatom frustules contain many metals at significant concentration, but diatom frustules have been assumed to be pure opal without any analytical proof by communities of relevant sciences. This is caused by difficulty in separating diatom frustules from silicate minerals chemically as well as physically. Alkaline leaching is a conventional method for determination of diatom opal and other biogenic silica, and uses difference of dissolution rate between diatom frustules and clay minerals. This involves somewhat tricky procedure: assuming that diatom frustules tend to dissolve easier than clay minerals, the critical timing, at which only diatom frustules are dissolved, are determined. Many improvements have been reported with respect to alkaline solution, temperature, and leaching time since 1950s (Berzukov, 1955; Hurd, 1973; Kamatani, 1980; Eggimann et al., 1980; DeMatser, 1979, 1981; Shemesh et al., 1988; Mortlock and Froelich, 1989; Müller and Schneider, 1993; Schluter and Rickert, 1998; Kamatani and Oku, 2000). There has never been a consensus regarding which method to be applied and different methods have been adopted depending on species, samples and locations (Kamatani, 2000).

Aim of the study is to investigate whether all elements in diatom frustules can be liberated by alkaline leaching. This study is implemented, because I suspect that some elements in diatom frustules are excluded unknowingly using the conventional analytical method.

5.2. Methods

5.2.1. Sediment trap samples

Sediment trap samples were collected at Station AB (53°5'N, 177°W, water depth 3197 m) in the Aleutian Basin of the Bering Sea and Station SA (49°N, 174°W, water depth 5406 m) in the central subarctic Pacific where primary productivity is extremely high. To collect the samples a PARFLUX Mark 7G-13 time-series sediment trap with 13 rotary collections was deployed approximately 600 m above the seafloor.

Two samples were chosen for the analyses from Station AB: one is collected in a low productive period (AB-20#6) and the other is in a high productive period (AB-19#1). One sediment trap sample collected at Station SA was also analyzed. This sample is characterized with abnormally high total mass flux and has a suspicion of volcanic ash mixing.

5.2.2. Compositional analysis

Settling particles separated from the formaldehyde storage solution by centrifugation were washed with ethanol and Milli-Q water and treated with 10 ml of 40% acetic acid solution at 40°C for 25 minutes. The supernatant solution was separated from residue (HAc residue) by centrifugation. After the solution was evaporated to dryness, HNO_3 solution and water were added [A]. Then, 10 ml of 3% hydrochloric acid was added to the HAc residue. The solution was separated by centrifugation and evaporated and HNO_3 solution and water were added [B]. The treatment with acetic acid and hydrochloric acid solutions is supposed to dissolve carbonates and oxides, respectively and the solutions [A] and [B] were named HAc and HCl fractions, respectively. To dissolve organic matter, 10% Hydrogen peroxide was added to the HCl residue and let the mixture in a sonicated water bath. The solution was also separated and

converted to an HNO_3 solution [C]. Alkaline leaching was performed against the hydrogen peroxide residue, which is supposed to consist of siliceous matter. 2M sodium carbonate solution was added and leaching was done at 80°C for 5 hours during sonication.

The supernatant solution was separated from residue and neutralized and prepared to HNO_3 solution [D]. The residue was washed with 0.5 N nitric acid because some of the liberated metals might be dissolved under the acidity condition. The separated solution was evaporated and converted to an HNO_3 solution [E]. The residue was freeze-dried and 10 mg of the dried sample was transferred to a Teflon vessel. One g of 68% nitric acid, 1 g of 70% perchloric and 1 g of 35% hydrofluoric acids were added to the vessel and the residue was decomposed completely by heating for 90 minutes. After evaporation, HNO_3 solution and water were added and the final solution was named HF fraction [F]. Three final solution (approx. 1 N HNO_3) were determined using inductivity coupled plasma mass spectrometry (ICP-MS; HP4500, Agilent Co., Ltd.). To avoid memory error by using a multi element standard solution at high concentrations, the calibration was carried out against a JB-3 decomposed solution with the known concentration of elements.

5.3. Results & Discussion

According to the dissolution kinetics, because opal flux is greater than 200 mg m^{-2} day^{-1}, siliceous fraction in AB-19#1 is considered to be unaltered diatom frustules with a negligible extent of contamination with clay minerals. Hence, Fractions of D, E, and F should pertain to diatom frustules. Fraction F is the most difficult one to dissolve and has been considered to be silicate minerals or clay by relevant science communities. Fig. 5.1 shows proportion of elements dissolved in the six fractions. In many elements, the amounts in F are much greater than those in

D+E. (Al, Ti, V, Cr, Mn, Fe, Y, Zr, Nb, and REEs). It is indicated that diatom frustules contain impurity in a state which cannot be dissolved by the conventional analytical method.

5.4. Conclusion

The conventional analytical method of diatom frustules using an alkaline solution is revisited and it is shown that the method fails to liberate most of metal elements and, therefore, tends to overlook most of metal elements in diatom frustules.

References

Berzukov, P L. (1955) Distribution and rare of deposition of silicate sedimentations in the Sea of Okhotsuk. *Dokl. Nauka SSR* **103**, 473-476

DeMaster, D. J. (1979) The marine budgets of silica and Si-32. Ph.D. dissertation, pp. 308, Yale University, New Haven.

DeMaster, D. J. (1981) The supply and accumulation of silica in the environment. *Geochim. Cosmochim. Acta* **45**, 1715-1732.

Eggimann, D. W., Manheim, F. T. and Betzer P. R. (1980) Dissolution and analysis of amorphous silica in marine sediments. *J. Sediment. Petrol.* **50**, 215-225

Hurd, D. C. (1973) Interaction of biogenic opal, sediment and seawater in the central equatorial Pacific. *Geochim. Cosmochim. Acta* **37**, 2257-2283.

Kamatani, A. (1980) Determination of biogenic silica in marine sediment. *La mer* **18**, 63-68.

Kamatani, A. and Oku, O. (2000) Measuring biogenic silica in marine sediments. *Mar. Chem.*

68, 219-229.

Kamatani, A. (2002) Measuring biogenic silica of marine samples: its situation and prospect. *J. Oceanogr. Soc. Japan* **9**, 143-159.

Mortlock, R. A. and Froelich, P. N. (1989) A simple method for the rapid determination of biogenic opal in pelagic marine sediments. *Deep-Sea Res. Part I,* **36**, 1415-1426.

Müller, P. J. and Schneider, R. (1993) An automated leaching method for the determination of opal in sediments and particulate matter. *Deep-Sea Res. Part I,* **40**, 425-444.

Schluter, M. and Rickert, D. (1998) Effect of pH on the measurement of biogenic silica. *Mar. Chem.* **63**, 81-92.

Shemesh A., Mortlock R. A., Smith R. J. and Froelich P. N. (1988) Determination of Ge/Si in marine siliceous microfossils: Separation, cleaning and dissolution of diatoms and radiolarian, *Marine Chemistry*, **25**, 305-323.

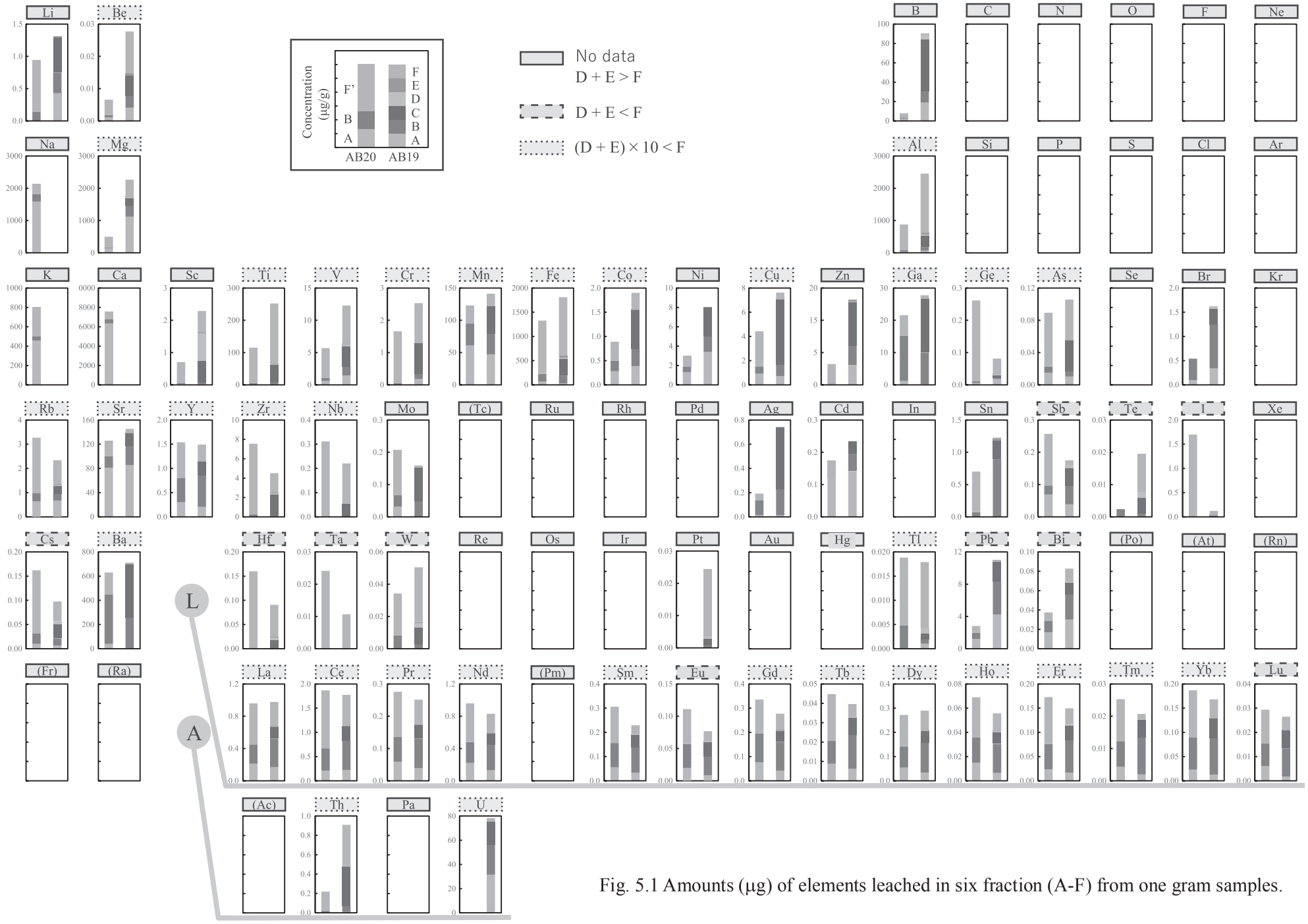

Fig. 5.1 Amounts (μg) of elements leached in six fraction (A-F) from one gram samples.

Conclusion

Elemental composition and chemical property of diatom frustules are investigated in this study. Siliceous fraction of settling particles contains various elements (Li, Be, Mg, Al, Sc, Ti, V, Cr, Fe, Co, Cu, Zn, Ga, As, Rb, Y, Zr, Nb, Sn, Sb, Cs, REEs, Hf, Ta, W, and Th) compared with the fractions of carbonate and oxide, and it is major carriers to transport those elements from surface water to sea floor (Chapter 2). Composition of siliceous fraction was assumed to be that of diatom frustules when opal flux is extremely high, based on the dissolution kinetics of aggregation. Elemental composition of diatom frustules determined by asymptote value for 51 elements was similar to, but significantly differs from, that of upper crust. A box model, in which alumino-silicates supplied to the surface water are assumed as sources of elements, could interpret the difference in concentrations from that of the upper crust as extent of recycled proportion from the deep water. The results indicate that diatoms digest alumino-silicates actively to obtain silicic acid (Chapter 3).

Observed ^{27}Al MAS NMR spectrum of sediment trap had the same characteristics as that of cultured diatom frustules and it is shown that state of aluminum in diatom frustules differ from clay minerals. That is strong evidence to show that contamination of clay minerals can be neglected. Moreover, the results show that high concentration of aluminum in siliceous fraction at low productivity caused by alternation of diatom frustules not due to contamination of terrigenous matter (Chapter 4). Most of the altered frustules cannot be dissolved by the conventional analytical method for diatom opal, and this result in overlooking of most of elements in diatom frustules (Chapter 5). The elemental cycles in the oceans must be reconstructed including diatom frustules as important carriers.